

1N-18
190200
38P

NASA Technical Memorandum 107610

Minimum Accommodation For Aerobrake Assembly- Phase II Final Report

Structural Concepts For A Lunar Transfer Vehicle Aerobrake Which Can Be Assembled On Orbit

John T. Dorsey, Judith J. Watson, and Robin D. Tutterow

October 1993

(NASA-TM-107610) MINIMUM
ACCOMMODATION FOR AEROBRAKE
ASSEMBLY. PHASE 2: STRUCTURAL
CONCEPTS FOR A LUNAR TRANSFER
VEHICLE AEROBRAKE WHICH CAN BE
ASSEMBLED ON ORBIT Final Report
(NASA) 38 p

N94-15446

Unclass

G3/18 0190200



National Aeronautics and
Space Administration

Langley Research Center
Hampton, Virginia 23681-0001



Introduction

There is continuing interest in manned exploration of the solar system, beginning with a return to the Moon and followed by a manned mission to Mars¹. The vehicles required for these missions are large and massive and cannot be placed in orbit by a single launch of the Space Shuttle (Space Transportation System [STS]) or a Heavy-lift Launch Vehicle. Multiple launches will place large components of the vehicles in orbit where the assembly and servicing will be conducted².

Large portions of the Lunar and Mars Transfer vehicle (LTV, MTV) masses consist of the propellant required for propulsive braking. Aerobraking, which uses aerodynamic drag forces created during a pass (aeropass) through a planetary atmosphere, can be used as an alternative to propulsive braking to achieve the reduction in velocity required to enter orbit around a planet. By reducing the amount of propellant required for a mission, aerobraking provides a potentially effective way to reduce the mass of LTV and MTV^{3,4}. To be viable, an aerobrake (as shown in figure 1) must be lightweight (its mass must be less than that of the propulsion braking system, including the propellant, it replaces), easily constructed on-orbit, reusable (in some cases), and have minimum packaged volume for transporting to low Earth orbit.

A multidisciplinary conceptual study was performed at the NASA Langley Research Center to define a reusable LTV aerobrake which could be assembled on orbit at Space Station Freedom (SSF). Major objectives of the study included: developing an aerobrake structural concept which could be assembled on orbit and would be compatible with thermal protection system (TPS) requirements, defining a TPS, identifying the infrastructure, automation, robotic, and manned Extravehicular Activity (EVA) requirements for assembling an aerobrake on-orbit, and identifying ground and flight experiments essential to the success of an aerobrake development program. This paper summarizes results from the conceptual structural design portion of the study.

Approach

The major objective of the conceptual structural design portion of the aerobrake study was to size an aerobrake structure, which along with the aerobrake TPS, would comprise no more than 20 percent (9040 lbm) of the LTV lunar return mass. The structure was also to be designed for efficient transportation to low earth orbit using either the STS or a Titan IV expendable launch vehicle (ELV), and for assembly on orbit.

To meet these objectives some of the conceptual design issues considered were; the segmentation of the aerobrake for packaging and on-orbit assembly, a joint design for assembly of the aerobrake, a structural design which included material selection and structural analysis with imperfection considerations, and the interaction between the TPS and the structure.

Three proposed segmentation concepts were evaluated for ease of packaging and assembly and one was selected for structural sizing. Two structural concepts were sized to withstand aerodynamic drag forces generated during deceleration into low-Earth orbit. The analysis yielded structural mass estimates for a set of materials. A joint design was proposed for assembly of the

aerobrake components and an estimated joint mass was determined. A TPS thickness was sized for each structural concept/material combination based on the thermal properties of the material and the thickness of the structure. Finally a mass estimate was made for each structural concept/material combination, including the TPS and joint mass.

This paper will discuss the aerobrake requirements and assumptions, the assessment of the segmentation concepts, a description of the two structural design concepts, the joint concept and assembly operations. Also the structural analysis and results, and an estimated mass for the aerobrake including TPS will be presented.

Assumptions and Requirements

This section summarizes the assumptions and requirements that were used in the present study for the conceptual design of the LTV aerobrake structure. The Earth-return portion of the LTV consists of two major components: the Payload/Avionics (P/A) module and the aerobrake (see figure 2). The target mass of the Earth-return LTV has been specified as 45,100 lbm, 20 percent of which (9040 lbm) represents the mass goal of the aerobrake. The P/A module has an octagonal cross section with a maximum diameter of 23.1 feet and a length of 22.0 feet. The P/A module is mounted to the leeward (concave) side of the aerobrake structure. The aerobrake structure is protected from aerodynamic heating on the windward side by the TPS. The aerobrake is a spherical cap with a base diameter of 50.0 feet and a radius of curvature of 44.55 feet. The spherical shape was chosen for the LTV aerobrake because its symmetry facilitates fabrication and on-orbit assembly and reduces operational support requirements. A partial toroidal skirt is attached to the outer edge of the spherical cap to prevent the protrusion of sharp aerobrake edges into the aerodynamic flow and increase the shielded volume in the aerobrake's wake. This skirt is a portion of a circular torus generated by rotating a 2-foot radius circle, which is tangent to the edge of the spherical cap, around the aerobrake centerline.

The interface between the P/A module and the aerobrake is a docking ring which enables the P/A module to separate from the aerobrake and land on the lunar surface while the aerobrake remains in lunar orbit. The diameter of the docking ring is assumed to be equal to the maximum diameter of the P/A module. The docking ring is restricted to a maximum depth of 3.28 feet (see figure 2) to prevent the aerodynamic flow behind the aerobrake from impinging on the P/A module. Detailed structural design and analysis of the docking ring were not included in this study.

No existing or currently planned launch vehicle has a payload shroud large enough to accommodate the fully assembled LTV aerobrake. Therefore, the aerobrake must be launched disassembled (figure 3) for assembly in low Earth orbit (LEO). To provide flexibility with respect to launch opportunities and payload manifests, the aerobrake subassemblies are sized to be transported to LEO by either the STS (15-foot diameter by 60-foot length cargo bay) or the Titan IV ELV (15-foot diameter by 66-foot length payload shroud) as described in reference 5. The assembly operations are designed to be accomplished by either EVA or robotic techniques, and are assumed to use the projected capabilities and utilities of SSF.

The TPS selected for use on the LTV aerobrake is an Alumina Enhanced Thermal Barrier (AETB) tile which has evolved from the high temperature LI2200 tiles that are currently used on the STS. The tiles are either bonded or mechanically attached to the structure. As the aerobrake structure deforms under load, gapping between the tiles or debonding of the tiles from the structure can occur. Therefore structural deformation constraints must be considered in the design. For this study a maximum tile dimension of one-meter was assumed and deformation constraints were based on shuttle tile gapping and debonding criteria.

The aerobrake surface pressure distribution at the time of peak stagnation pressure during a nominal aerobraking trajectory was chosen as the design loading for the present study (see figure 4). This pressure distribution is non-uniform because the angle of attack for the nominal trajectory is 11 degrees. The maximum stagnation pressure is 0.737 psi and is associated with a maximum LTV deceleration value of 4.18 g's.

Concept Descriptions

Aerobrake Segmentation Concepts

The three segmentation concepts evaluated in this study are the longitudinally sliced panels, the core-petal panels and the hexagonal panels (see figures 5 through 7). The core-petal and the sliced panels concepts were previously proposed in reference 5 as part of phase one of the aerobrake study, and the hexagonal panel concept was developed during this study, phase II. The panel sizes for the three concepts are dictated by the launch vehicle cargo-bay cross-sectional dimensions, the location of the docking ring attachment points, and compatibility with the rib intersections of an isogrid pattern. The seams of the aerobrake segments were defined by projecting the intersection points of an isogrid pattern in the base plane onto the spherical surface of the aerobrake, and connecting the projected points by arc segments of great circles. These panel seams have curvature in one direction only, which simplifies line joint manufacturing and on-orbit assembly of the panels.

The attachment points of the docking ring were required to be located away from the panel seams. These attachment points were located on the structure at a radius of 25 feet from the aerobrake center and at isogrid rib intersection points.

The three segmentation concepts were given a cursory assessment based on launch vehicle packaging, ease of assembly, number of parts, a preliminary mass estimate and compatibility with SSF systems for storage and manipulation. Of these five concerns, launch vehicle packaging and ease of assembly were determined to be the major discriminators for determining the preferred segmentation concept.

Early in the assessment of the segmentation concepts it was shown that the longitudinally sliced panel segmentation concept, shown in figure 5, would not meet the packaging requirements. The concept consists of five longitudinal panels with three different geometric shaped panels. The panels are sized to be of equal width, 10 feet, with the docking ring attachments located on the interior of the three center panels. The aerobrake skirt section is included on the perimeter edge of

each panel. From figure 5 it can be seen that the panels can not be packaged within the 15 foot diameter of the cargo bay area of either the STS or Titan IV. Since the panels can not be packaged in either launch vehicle this segmentation concept was eliminated from further consideration in the study.

The core-petal panel segmentation concept shown in figure 6 consists of a center or core hexagonal panel ringed by 12 petal panels. The panels are sized so the docking ring attachments are located on the interior of the petal panel geometry and occur at rib intersection points. The core-panel has a planform dimension of 9.8 feet across the vertices and 8.4 feet across the flats. The petal panels have a maximum planform dimension of 12.5 feet by 20.7 feet. The aerobrake skirt section is included on the perimeter edge of each petal panel. As shown in figure 6 the core-petal panels can be packaged in the STS cargo bay by laying the petal panels lengthwise so that they overlap one another. The core panel is packaged on edge as was done with the hexagonal panels. This packaging configuration requires 50 feet of the cargo bay length and does not account for packaging supports or stowage canisters.

The hexagonal panel segmentation concept shown in figure 7 consists of 19 hexagonal or truncated hexagonal (at the perimeter) panels in a two-ring pattern. There are four different geometric shapes: the center panel, the first-ring panels, and two shapes in the second-ring panels. The panels are sized so the centers of the first ring of the panels are 12.5 feet from the center of the aerobrake. This allows the docking ring attachments to be made in the center of the panels. The panels have the maximum planform dimensions of 14.4 ft across the vertices and 12.5 ft across the flats. The aerobrake skirt section is included on the perimeter edge of each second-ring panel. As shown in figure 7, the hexagonal panels (including the skirt section and allowing for spacing between the panels) can be stacked in a 25 foot length of the STS cargo bay. This arrangement does not account for a stowage cannister.

Between the hexagonal panels and the core-petal panels the hexagonal panels were considered the better concept for packaging in the STS or Titan IV ELV cargo bays. The hexagonal panels were shown packaged in less than half of the cargo volume, including spacing for supports. (It will be shown later that the panel and TPS thickness will be about 5 inches thick.). This packaging arrangement allows for other hardware/equipment to be launched with the aerobrake panels if desired. The core-petal panels require the majority of the cargo bay volume, not including spacing for supports.

The other discriminator, ease of assembly, relates to the handling of the panels during assembly. If all the panels were the same size then it follows that more panels will take longer to assemble. However, if the panels are different sizes then the ability to maneuver a panel during assembly can be effected to the point that a larger number of smaller panels could potentially be assembled quicker and easier than a few larger sized panels. Such is the case with the hexagonal panels versus the core-petal panels. The hexagonal panel concept has six more panels to assemble than the core-petal concept (19 versus 13 panels), but the hexagonal panels are significantly smaller therefore were considered more maneuverable than the core-petal panels. Also because of their size the hexagonal panels had shorter length seams to align and join together than those of the core-petal panels. For these reasons the hexagonal panels were chosen as the preferred segmentation concept.

Structural Concepts

Two different structural concepts (sandwich and isogrid) were studied in order to identify a low mass aerobrake structural design. This section describes the structural concepts and material options evaluated in the study.

Sandwich Shell Sandwich construction, which features a lightweight honeycomb core and thin, high stiffness face sheets (see figure 8a), was considered for the aerobrake structure because it provides high flexural stiffness at low areal density. Composite face sheets were assumed to have a mid-plane symmetric, quasi-isotropic lay-up. The primary consideration for sizing the sandwich stiffness will be resistance to global shell buckling due to applied pressure. To accommodate TPS requirements, local deflection and radius-of-curvature limits may also be important.

Isogrid Shell A thinner sandwich shell stiffened with an isogrid arrangement of ribs (as shown in figure 8b), was considered because it can also result in lightweight and efficient structures⁶. The isogrid pattern has ribs which are oriented at 0, +60, and -60 degrees, as shown in figure 8b, and gives the shell globally isotropic membrane stiffness. The rib spacing is determined from the same projected isogrid pattern that defines docking ring attachment points, and panel seams. In the present study, the ribs are assumed to be I-beams. In an isogrid design, the ribs are designed to carry most of the loading; thus, when composite materials are used for the ribs, a lay-up which maximizes the longitudinal stiffness is desirable. The rib design chosen, a $[+45, -45, 0_n]_s$ lay-up, uses a pair of ± 45 -degree outer plies to stabilize the 0-degree plies which run along the longitudinal axis of the rib. Both uniform and sandwich construction skins were investigated for the isogrid structure. As before, composite skins were assumed to be mid-plane symmetric and quasi-isotropic. Similar to the sandwich concept, the primary consideration for sizing the isogrid ribs is resistance to global buckling of the shell. Prevention of local buckling of the skin between the ribs, as outlined in reference 6, will dominate the skin design. However, local deflection and radius-of-curvature limits imposed by the TPS must also be considered

Materials Because the aerobrake operates in a high temperature regime and is mass critical, materials with high specific stiffness which can also operate at elevated temperatures are needed. Five candidate materials were evaluated in the present study. The candidates, with properties listed in Table 1, are aluminum, titanium, silicon carbide (particles)-aluminum (SiCp/Al), graphite-epoxy (Gr/E), and Graphite Polyimide (Gr/PI). Specific stiffness range from a high of 529×10^6 inches for the uni-directional Gr/E to a low of 102×10^6 inches for aluminum, and the maximum operating temperature ranges from a low of 260° F for Gr/E to a high of 750° F for titanium. Each of the materials was used to size aerobrakes for the sandwich structure concept, and three of the materials, aluminum, SiCp/Al, and Gr/E, were used to size aerobrakes for the isogrid structure. However, in the subsequent sections which discuss the analysis in detail, the Gr/E material results will be presented as representative of all the material cases.

Aluminum and titanium were the two metals investigated for this study. The aluminum would probably be the least expensive of the materials to use, however it has the lowest specific stiffness and a low-to-mid range operating temperature. Titanium had the highest operating temperature of the materials selected. This property could allow the thickness of the TPS required to be reduced

and thus lower the TPS mass. The disadvantages of the titanium are that it can be expensive and difficult to machine. Its specific stiffness is identical to that of aluminum.

SiCp/Al is a metallic composite material which has a higher specific stiffness ratio than aluminum and titanium. Although SiCp/Al is reported to have an operating temperature of 500° F, experts recommend that the actual operational temperature be limited to approximately 350° F. Further investigation would be required to determine if the higher operating temperature would be acceptable. Since SiCp/Al currently can not be manufactured as a honeycomb material, the SiCp/Al sandwich structure in this study was comprised of an aluminum honeycomb core with SiCp/Al facesheets.

Gr/E and Gr/PI were two composite materials investigated for this study. Gr/E is a commonly known composite with a high specific stiffness ratio and high strength. It also had the lowest operating temperature (260° F) of the five candidates. However, reference 8 indicates that for short term use and a dry thermal environment the Gr/E could operate at a temperature of 350° F. For this study both the 260° F and the 350° F thermal environments were considered since the aerobrake operates in space and experiences a short, high temperature environment. Gr/PI is a high temperature composite material. Its specific stiffness ratio is not as high as Gr/E but it is higher than the metals. The Gr/PI material used in this study is based on a Gr/PI with a newly developed resin, LaRC-RP46⁹. This material is capable of duplicating the properties of current Gr/PI but with a higher operating temperature. However the material would need more development work and verification of its capability. Also Gr/PI composites are known to have exhibited problems with micro-cracking during processing and use which would have to be taken into consideration in the design process.

Joint Concept

The joints required to assemble the aerobrake panels must not only provide sufficient strength and stiffness for the aerobrake to function as a continuous structure, they must also seal the seams between the panels to prevent hot gas flow through the aerobrake. In addition the joints must be compatible with EVA astronaut or robotic assembly. To minimize the number of parts handled, the joints should have captured fasteners.

The joint concepts considered herein are based on a quick-attachment joint developed for on-orbit assembly of large space trusses by astronauts during EVA¹⁰. Two joints are needed for assembling the aerobrake panels. The line joint shown in figure 9 is used to join sandwich panels at the seams. The node-joint shown in figure 10 is used to join isogrid rib intersections.

Both joint concepts consist of two matching halves which include tapered tongues and grooves. The tongue and groove feature allows easy insertion of the joint halves, and a continuous load path across the joint. For the line joint, the tongues and grooves are wedged together removing the free-play and sealing the seams between the panels. A drogue-capture feature (not shown in the figure) is incorporated into the joint to aid in aligning the panels and then holding the panels together while the joint is being locked. The ribs are joined together by a node which is inserted at the rib intersection. The end of the ribs and the node have the same type of tongue and groove arrangement as the line joint. The rib joint connection is made after all line joints common

to the rib intersection have been assembled. As shown in figures 9 and 10, captured bolts are used to lock all the joint halves together. This feature reduces the number of parts that must be managed during assembly thus simplifying the closure operation. Both joint concepts were also assumed to be 7075-T73 aluminum alloy. To reduce the mass of the line joint some of the joint material was removed and replaced with the core honeycomb material.

Assembly Scenario

The aerobrake assembly was to be accomplished using either EVA astronauts with robotic assistance or robotics alone. With both assembly methods, the aerobrake can be assembled from the SSF as illustrated in figure 11. If necessary, the aerobrake could also be assembled out of the STS cargo bay in a similar fashion. The components are stowed in canisters near the assembly site. The aerobrake is assembled in rings, beginning with the center panel which is attached to a turnstile and rotated to allow subsequent panels to be attached. Because the panels of the aerobrake overlap, they are assembled by being brought in alternately from the back and the front of the structure. Thus, all of the edges of a single panel will not have the same line joint orientation. The rib node joint will be attached at all rib intersections along the seams after all the adjoining panel line-joints are assembled. For assembly by EVA astronauts with robotic assistance, the Space Station Remote Manipulator System (SSRMS) retrieves aerobrake panels from their stowage canisters and positions them within reach of the EVA astronauts. The astronauts, positioned by an auxiliary mobile transporter with positioning foot restraints, take the panels from the SSRMS and align and mate the panels with adjacent panels on the turnstile. After the astronauts have assembled the aerobrake, the Special Purpose Dexterous Manipulator (SPDM) tightens all of the captured bolts. For the robotic assembly scenario the SPDM would be used to align and mate the panels.

Structural Analysis

Models

A finite element model was constructed of the aerobrake for analysis and structural sizing. The mesh was chosen to incorporate features of both the sandwich and the isogrid structural concepts so that only one model was required. The resulting finite element mesh, composed of triangular plate (bending plus membrane) elements, is shown in figure 12. Node points are included along the boundaries of the hexagonal panels so that loads and stresses at the joints between the panels can be obtained. Node points have also been located along the ribs of the isogrid structural concept with rib spacing equal to the edge length of the hexagonal panels as shown in the figure. The finite element mesh uses six elements along the edge of a triangular cell formed by the ribs which is sufficiently refined to capture the second skin buckling mode between the isogrid ribs (reference 6).

The six support points shown with circles represent the docking ring attachment points for the isogrid structural concept. These are the only six points that meet the requirements that the support points be located at a rib intersection and not on a panel boundary. However, a major advantage of the sandwich structural concept is that since it has no ribs, the P/A module can be continuously supported by the shell leading to a much better distribution of the interface loads and potentially a

lighter structure. The mesh shown in figure 12 does not have sufficient fidelity to model this continuous support condition. However, six additional supports (giving a total of 12) could be located on the model at panel boundaries, as indicated by the squares in the figure, to study the performance benefits that could be achieved by using additional supports.

The non uniform pressure loading applied to the aerobrake is illustrated in figure 4. A factor of safety of 1.4 was used for all analyses and was applied to the pressure loading. Since the buckling load of spherical caps (like the aerobrake) under external pressure is very sensitive to small deviations (or imperfections) from the ideal shape¹¹, relatively small structural imperfections can lead to large reductions in the buckling load. Thus, even at the conceptual level, buckling sensitivity to imperfections should be taken into account when sizing aerobrake shell structures. An approximate method for considering imperfection sensitivity in the design process is described in the next section.

Sandwich Structure

Analysis Procedure A simple reduced stiffness method, that provides a basis for designing shells which are sensitive to imperfections, is described in reference 12. There, the following formula is proposed for calculating the buckling load of a shell with imperfections,

$$p_{c,m}^* = \frac{U_{B,m}}{(U_{B,m} + U_{M,m})} p_{c,m} \quad (1)$$

where $p_{c,m}$ is the classical critical pressure for buckling mode m , $U_{B,m}$ and $U_{M,m}$ are the bending and membrane strain energies in the associated critical mode. Although additional research is needed to establish the validity of this approach, it was assumed to be satisfactory for conceptual design purposes and was used in the present study.

Results from a preliminary study of the sandwich concept, using a coarser mesh than that shown for the aerobrake in figure 12, showed a difference of 7.6 percent between the buckling load predicted by a linear bifurcation analysis and a nonlinear analysis of a perfect spherical cap supported at six points. Thus, the linear bifurcation analysis¹³ was considered to be accurate enough for conceptual design purposes. To design the aerobrake to account for imperfections, several buckling modes are calculated, the amount of bending and membrane strain energy is calculated for each mode, then the reduced critical load is calculated using equation (1). The reduced critical load is used as the aerobrake design load.

Initially, the sandwich face sheet and core thicknesses are sized to obtain sufficient bending stiffness to resist buckling at the design pressure. The bending stiffness of a sandwich shell is

$$D = \frac{E_f t_f t_c^2}{2(1 - \nu_f^2)} \quad (2)$$

where E_f and ν_f are the modulus and Poisson's ratio of the face sheet, t_f is the face sheet thickness, and t_c is the core thickness. The areal density of a sandwich shell is given by

$$\left(\frac{M}{A}\right) = 2 \rho_f t_f + \rho_c t_c \quad (3)$$

where ρ_f and ρ_c are the densities of the face sheets and core respectively. A minimum mass sandwich design can be obtained by solving equation (2) for t_c , substituting that expression into equation (3), and setting the partial derivative with respect to t_f of the resulting expression equal to 0. This results in the following expression for the face sheet thickness of a minimum mass design,

$$t_{f,mm} = \frac{1}{2} \left[\left(\frac{\rho_c}{\rho_f} \right)^2 \frac{(1 - \nu_f^2)}{E_f} D \right]^{1/3} \quad (4)$$

Initial analyses were used to determine a value of D sufficient to prevent buckling at the design pressure. Then, equations (4) and (2) were used to obtain initial estimates for sandwich shell core and face sheet thicknesses that approximate a minimum mass design. Since these values do not consider the beneficial effect of the shell membrane stiffness on buckling, using these values results in an over-designed structure (the shell buckles at a load which is greater than the design load). Further refinement in the design, and thus, less mass, was obtained by using the linear bifurcation buckling analysis to size the structure (as described in the next section).

Results The fundamental buckling mode for the sandwich aerobrake supported at the six points shown in figure 12 has three circumferential waves. The percentage of the total strain energy associated with bending represents a knock-down factor which takes into account buckling sensitivity to initial imperfections (see equation 1). Its value ranged between 53 and 55 percent for the sandwich panel with graphite epoxy face sheets, and the reduced critical load was equal to the design load when

$$t_c t_f = 0.076 \quad (5)$$

When equation (5) is solved for t_c , and the result is substituted into equation (3), the areal mass of the sandwich design becomes a function of a single parameter, t_f , as shown in figure 13. Minimum mass for the sandwich, .0094 lbm/in², is achieved for $0.035 \leq t_f \leq 0.04$ inches. The value of 0.04 was chosen for the design because it requires a thinner core (1.90 versus 2.17 inches) and, thus, leads to a thinner structure which packages more efficiently for launch. (Values of t_c and t_f calculated for minimum mass designs for the other materials are listed in Table 2.)

When the number of supports on the sandwich aerobrake is increased from 6 to 12, a minimum mass design is achieved when t_c is 1.84 inches and t_f is 0.034 inches. The resulting mass for the 12-support case is 9.5 percent less than in the 6-support case (see Table 3). Further reductions in the sandwich aerobrake mass could be expected in the case of continuous support representing for example, a continuous docking ring bonded to the aerobrake structure. The imperfection related knockdown factor on buckling is 4 percent smaller for the 12-support design than for the 6-support design.

A maximum TPS tile size of 39.37 inches is used for this study. The structural deflection over a 39.37 inch reference length is not allowed to exceed 0.1 inches to insure that the tiles do not

debond. These values lead to a requirement that the minimum allowable radius-of-curvature from elastic deformation be 1938 inches for the structure. A contour plot of the displacements in the x-direction (see figure 12 for axis orientation) for the Gr/E sandwich aerobrake (with 6 supports, t_c of 1.9 inches, and t_f of 0.04 inches) subjected to the design pressure is shown in figure 14. The maximum out-of-plane (x) displacement is 1.24 inches and occurs on the aerobrake leading edge. The deflection contour plot shows that the most rapid change in deflections, and thus, the greatest amount of induced curvature, occurs near the support points. The radius-of-curvature induced by the deflections in the sandwich aerobrake is calculated to be 2606 inches using equations found in reference 12. Since this is above the minimum allowable of 1938 inches, the TPS deflection criteria is met by the sandwich structure.

Stresses in the graphite epoxy face sheets for the sandwich design (with 6 supports, t_c of 1.9 inches, and t_f of 0.04 inches) were also checked for acceptability. In reference 7, representative values of ultimate stress in a quasi-isotropic lay-up are given for a high-modulus graphite epoxy system (P75/1962) of the type considered for this study. Ultimate stress values used in the present study were 45×10^3 psi in tension, and 27×10^3 psi in compression for a quasi-isotropic lay-up. The maximum and minimum average nodal stresses in the face sheets were 44.2×10^3 and -37.0×10^3 psi respectively. The peak tensile and compressive stresses occur locally at the supports, as shown by the stress contour for the radial stress, σ_r , in figure 15a, whereas most of the skin is in a very low stress state. Although the peak compressive stress is greater than the material ultimate, the design can be made acceptable without adding significant mass to the aerobrake by locally stiffening the support region because the stress reduces to an acceptable level in less than one sixth of the panel radius (see figure 15b).

Isogrid Structure

Analysis Procedure Predicting buckling in an isogrid structure under transverse pressure loading generally requires nonlinear analysis for two reasons. First, because prebuckling deformations are important, a linear bifurcation analysis is not valid for this design problem^{6,13}. Second, the first buckling mode predicted by the bifurcation analysis is not a buckling mode for this structure-loading combination; buckling actually occurs at the second mode⁶. A lightweight isogrid design features thin skins; hence local skin buckling between the ribs must be considered in addition to the global instability, as described in reference 6, if a lightweight design is desired. Thus, in this study, geometrically nonlinear analysis is used to size the isogrid aerobrake concept. Although no attempt is made here to determine the imperfection sensitivity of the isogrid design, the same knock-down factor (54 percent) determined for the sandwich design is applied in the analysis of the isogrid design for comparison.

After the isogrid structure was sized to meet the buckling criteria, the stresses in the skins and ribs were checked for acceptability. Since preliminary studies showed that the isogrid aerobrake was unnecessarily heavy when a uniform skin was assumed, sandwich construction was chosen for the isogrid skins. For the results which follow, the skins had graphite-epoxy face sheets and aluminum honeycomb core, and the ribs were also made from graphite-epoxy. Ultimate stresses for the face sheets (quasi-isotropic lay-up) were given in the section on sandwich results. The ultimate strength of the ribs was assumed to be the longitudinal strength of a unidirectional lay-up of P75/1962⁷ which is 124×10^3 psi in tension and 63×10^3 psi in compression. As with the

sandwich panel, stresses which exceeded ultimate values were allowed only in a localized region surrounding the supports.

Results A Gr/E isogrid aerobrake design which met the buckling and stress requirements had the following properties. The skins had a core thickness of 0.894 inches and a face sheet thickness of 0.023 inches. The ribs had a width of 2.0 inches, height of 2.7 inches, web thickness of 0.1 inches and flange thickness of 0.35 inches, resulting in a rib area of 1.6 in² and a moment of inertia about the primary bending axis of 2.01 in⁴. (The skin core and facesheet thickness dimensions calculated for minimum mass designs for the other materials are listed in Table 4.) A contour plot of the displacements in the x direction for the Gr/E isogrid aerobrake is shown in figure 16. The maximum out-of-plane displacement for this configuration with 6 support points is 1.48 inches and occurs on the aerobrake leading edge. For the associated deflection shape, 54 percent of the strain energy is in the ribs and 46 percent is in the sandwich skins. Normally in an isogrid structure, the majority of the loading is carried by the ribs. However, in the aerobrake structure, nearly half the load is carried by the skin because the skin must be relatively stiff to resist buckling.

The greatest change in curvature in the isogrid structure occurs near the support points. The minimum radius-of-curvature induced by the deflections is 2338 inches along a rib, and 700 inches in the center of a skin between ribs. Since the radius-of-curvature in the center of the skins is smaller than the TPS requirement of 1938 inches, local stiffening of the skin would be required in critical areas near the supports. However, the additional mass required to make the TPS and isogrid structure compatible were not addressed in this study.

Stresses in the graphite epoxy sandwich skin face sheets and the graphite epoxy ribs were also checked for acceptability (with ultimate stress values for both cited previously). The maximum and minimum average nodal stresses in the isogrid skin face sheets, 41.5×10^3 and -8.8×10^3 psi respectively, occurred locally at the support points as for the sandwich design (see figure 17 for a typical skin stress distribution for σ_T). The maximum compressive stress in a rib, which is not local to a support point, was 64.4×10^3 psi. Although this value is slightly higher than the ultimate (63×10^3 psi), it occurred over a small area. Thus, reducing the stress to an acceptable level would not add much mass, and no attempt was made to reduce the stress any further in this study. The maximum compressive rib stress near the support points is 83.6×10^3 psi. As with the sandwich design, the ribs could be stiffened in the support point region to reduce stresses to an acceptable level without adding significant mass.

Line Joints Results

Analysis of the aerobrake sandwich structural configuration shows that the maximum line joint load, tangent to the shell and perpendicular to the line joint, is about 10,000 lbf/in. However, since the line joint depth is assumed to be equal to the thickness of the sandwich shell, the mass of the line joints should be different for the different shell material cases. To estimate the line joint mass, the joint shown in figure 9 is sized for 2-inch and 4-inch depth such that it sustains a net section stress corresponding to two times the maximum line joint load of 10,000 lbf/in. From this preliminary joint sizing, the 2-inch and 4-inch joint cross-sections were determined to have cross-sectional areas of 2.182 in² and 5.228 in² for the joint material and 1.818 in² and 10.772 in² for

the honeycomb material, respectively. Since the maximum line load, 10,000 lbf/inch, is the same for both joint sizes, the minimal thickness of the aluminum joint material is 0.268 inches for both joints. This thickness is based on an ultimate strength value of 75.0×10^3 psi for 7075-T73 aluminum alloy.

TPS Sizing

For a low-mass, high-stiffness design, the structural and TPS materials must be selected as a system. The material properties (stiffness, density, etc.) and material operating temperatures must be assessed in combination with the required TPS thickness to determine the structural-TPS system with the lowest mass. A one-dimensional, analytical study was performed to determine the TPS thickness required for each of the material candidates for both the sandwich structure and the isogrid structure. Results from the study are listed in tables 2 and 4.

Table 2 presents the results for the sandwich structure and Table 4 presents the results for the isogrid structure. The tables list the core and face sheet thicknesses (the rib dimensions are not presented since they are not used in the TPS analysis), the maximum allowable temperatures for each material, and the resulting TPS thickness for the sandwich panels and the isogrid panel skins. As indicated in table 2 and 4, except for Gr/E, the TPS thickness required (and thus mass) for all cases was the same. This thickness (.6125 inches) is the TPS minimum gauge thickness. Since all materials except for the Gr/E require minimum gauge thickness, the temperature is not a discriminator in the use of the materials, other than Gr/E.

Total Mass

The total mass of the aerobrake structural system consists of the structure, joints, TPS and TPS attachment systems. The structural masses of the sandwich concept and the isogrid concept skin were based on a total aerobrake surface area of 354,122 in². The sandwich core density was chosen as .00231 lbm/in³ (4 lbm/ft³) for all materials. The isogrid rib mass was based on the cross-sectional area of the ribs, the material density, and a total rib length of 15,860 inches.

An attempt was also made to estimate the mass of the joints in the aerobrake structure. The mass of the sandwich concept line joint was determined by using the cross-sectional areas of the joints discussed in the previous section. By using a linear interpolation between the two-inch and four-inch sized joints, a cross-sectional area for the joint could be determined which included the amount of cross-sectional area attributed to the solid joint area and the honeycomb-filled area. The joint fasteners are assumed to be distributed along the seam at every 12 inches. At the joint fastener location the joint was assumed to be solid 1-inch along the seam on either side of the fastener to allow enough material for the fastener. The mass of the structure that the joint replaced was subtracted from the structural mass. Table 5 shows the resulting structural mass, the joint mass and the TPS mass for the sandwich structure material cases.

For the isogrid structural concept, masses were determined for the skin line joints and the rib joints. Because the skin line joints were too thin for use of the linear interpolation between the two-inch and four-inch joint designs, an approximate cross-sectional area was used maintaining the

.268 in. minimal thickness from the sandwich concept line joint as a reference thickness. The minimal thickness dimension of .268 in. was reduced by the percent of total strain energy carried by the ribs under the applied pressure load (since the skin face sheets were no longer carrying the total load). This new dimension was used to calculate solid joint and hollowed honeycomb cross-sectional areas for each material candidate. The skin line-joint mass was then determined in the same manner as the mass of the sandwich concept line joint. The rib joint mass was calculated from the determined geometry of the joint. Again the mass of the structure that the skin and rib joints replaced was subtracted from the structural mass. Table 6 shows the resulting structural mass, the joint mass, and the TPS mass for the isogrid structure material cases.

The total mass of the aerobrake structure is a sum of the structural mass, joint mass and TPS mass and is listed in the next to last columns of Tables 5 and 6. The aerobrake mass as a percentage of the LTV Lunar return mass is listed in the last columns. Five configurations which met the 20 percent mass goal were sized. The sandwich concepts, using either the SiCp/Al or the Gr/E materials, and all the isogrid material concepts had predicted masses of 17-20 percent of the LTV mass.

Concluding Remarks

A multidisciplinary conceptual study was performed to define a reusable Lunar Transfer Vehicle (LTV) aerobrake which could be assembled on orbit at Space Station Freedom. This paper described the aerobrake segmentation concepts, structural concepts, a joint concept for assembly of the aerobrake, a structural design which included material comparisons and structural analysis with imperfection considerations, and the sizing of the TPS.

The major goal of the present study was to determine if an integrated structure/TPS system could be designed having a mass which is less than 20 percent (9040 lbm) of the LTV lunar return mass. Aerobrakes using both the isogrid and sandwich structural concepts with associated TPS systems, were sized which met this goal. The isogrid aerobrake mass was slightly less than the sandwich design for all of the materials considered.

Results from this study show that a 50-foot-diameter LTV aerobrake can be designed for on-orbit assembly, and can also be efficiently packaged for transporting to low Earth orbit aboard the Space Shuttle Transportation System. An erectable line joint concept, which is lightweight and amenable to on-orbit EVA and robotic construction methods has been described. This joint concept is based on the erectable space station joint and includes important assembly features such as self-contained attachment mechanisms and a joint capture feature. Additional design and analysis are needed to characterize the strength, stiffness, and structural linearity of the joint concept and to better estimate its mass.

Since small structural imperfections can seriously degrade the predicted buckling performance in shell structures such as the LTV aerobrake, structural sizing, even at the conceptual design phase, must take the effect of these imperfections into account. A reduced stiffness method for designing shells which are sensitive to initial imperfections was used to design the sandwich LTV aerobrake. For comparison, the same method was used to size both aerobrake structural concepts.

Although the reduced stiffness method provided a theoretical approach to design the aerobrake structure, more research is needed to assess the validity of this method and its applicability to the aerobrake problem.

References

1. Report of the National Commission on Space: Pioneering the Space Frontier. Bantam Books, Inc., 1986.
2. Mikulas, Martin M., Jr.; and Dorsey, John T.: An Integrated In-Space Construction Facility for the 21st Century. NASA TM-101515, 1988.
3. Walberg, Gerald D.: A Review of Aerobraking for Mars Missions. Paper No. IAF-88-196, Oct. 1988.
4. Braun, Robert D.; and Blersch, Donald J.: Propulsive Options for a Manned Mars Transportation System. AIAA-89-2950, July 1989.
5. Katzberg, Stephen J.; Butler, David H.; Doggett, William R.; Russell, James W.; Hurban, Theresa: Aerobrake Assembly with Minimum Space Station Accommodation. NASA TM-102778, October 1990.
6. Dorsey, John T.; and Dyess, James W.: Structural Performance of Two Aerobrake Hexagonal Heat Shield Panel Concepts. NASA TM-4372, May 1992.
7. Rawal, S. P.; Misra, M. S.; and Wendt, R. G.: Composite Materials for Space Applications. NASA CR-187472, August 1990. (Performed by Martin Marietta Astronautics Group under contract NAS1-18230.)
8. DOD/NASA Advanced Composites Design Guide, Vol. 1, Design. First edition. Structures/Dynamics Division, flight Dynamics Laboratory, AF Wright Aeronautical Lab., Wright-Patterson Air Force Base, Ohio; Prepared under contract F33615-78-C-3203 by Rockwell International Corporation, North American Aircraft Operations. July 1983.
9. Pater, R. H.: The 316^o C and 317^o C Composite Properties of an Improved PMR Polyimide: LaRC-RP46. Presented at the 36th International SAMPE Symposium, San Diego, Ca., April 15-18, 1991.
10. Heard, Walter L. Jr.; Bush, Harold G.; Watson, Judith J.; Spring, Sherwood C.; and Röss, Jerry, L.: Astronaut/EVA Construction of Space Station. AIAA paper no. 88-2454, presented at AIAA SDM Issues of International Space Meeting, Williamsburg, Va., April 21-22, 1988.
11. Bushnell, David: Computerized Buckling Analysis of Shells. Kluwer Academic Publishers, c.1989.

12. Zintilis, G. M.; and Croll, J. G. A.: Pressure Buckling of End Supported Shells of Revolution. *Journal of Engineering Structures*, Volume 4, No. 4, October 1982.
13. Brush, Don O.; and Almroth, Bo O.: *Buckling of Bars, Plates, and Shells*. McGraw-Hill, Inc., c.1975.

Table 1. Material Properties

Material	E x 10 ⁶ psi	ρ lb/ft ³	E/ρ x 10 ⁶ in	ν	F _{ult} ksi	Maximum Temperature °F	Comments
Aluminum ⁷ 7075-T6	10.3	.101	102	.33	76	350	
Titanium ⁷ Ti 6Al-4v, α- β (weldable)	16.4	.16	102.5	.31	130	750	Difficult to machine
SiCp-Al ⁷ 2124-T6 35% v/o	20.4	.104	196	.25	95T 103C	350-500**	Used only for skin and ribs. Can not manufacture honeycomb. Use aluminum for core of sandwich.
Graphite Epoxy ⁷	14.4 iso 33.3 uni, E1	.063	228 529	.321 .738	44 63	260-350†	Sandwich panel size may be approaching limit of manufacturing capability.
Graphite Polyimide ^{7,††}	8.2 iso	.057	144	.34	76T 52C	500-600	Possible microcracking problem

Where E is the modulus of elasticity, ρ is density, ν is Poisson's ratio, and F_{ult} is ultimate strength.

** Has been tested for 500 °F, but is recommended for use at 350 °F or below.

† Typically used at a max. temperature of 260 °F, but for a short dry pass can go to 350 °F⁸.

†† A graphite-polyimide with a resin LaRC-RP46, which can match the strength properties of graphite polyimide T300/580 but has a higher maximum temperature capability⁹.

Table 2. Sandwich Structure and TPS Sizing Results

Material	Core depth in	Face sheet thickness in	Maximum allowable temperature oF	Resulting TPS thickness in	Area TPS mass including attachments lb/ft ²
Aluminum	3.017	.0315	350	.6125	1.628
Titanium	3.024	.0196	750	.6125	1.628
SiCp-Al	2.139	.0238	350	.6125	1.628
Graphite Epoxy	1.9	.04	350 260	.7995 .9875	1.815 2.003
Graphite Polyimide	2.522	.049	550	.6125	1.628

Table 3. Influence of Number of Supports on Aerobrake Mass

	6 Supports	12 Supports
t core	1.90	1.84
t facesheet	0.04	0.034
λ_1	1.871	1.985
λ_1^*	1.005	0.993
(M/A), lbm/.in ²	0.00943	0.00853
Total mass, lbm	3339.	3021. (-9.5%)

Table 4. Isogrid Structure and TPS Sizing Results

Material	Core depth in	Face sheet thickness in	Maximum allowable temperature of	Resulting TPS thickness in	Area TPS mass including attachments lb/ft ²
Aluminum	1.5	.02	350	.6125	1.628
SiCp-Al	1.093	.02	350	.6125	1.628
Graphite Epoxy	.894	.02	350 260	.8125 1.0375	1.828 2.053

Table 5. Aerobrake total structure mass and TPS mass for a sandwich structure.

Material	Face sheet density lb/in ³	Face sheet thickness in	Core depth in	Structure mass lb	Joint mass lb	TPS mass lb	Total aerobrake mass lb	% of LTV total mass
Aluminum	.101	.0315	3.017	4560	1844	4003	10407	23.0
Titanium	.16	.0196	3.024	4535	1829	4003	10367	23.0
SiCp-Al	.104	.0238	2.139	3418	1115	4003	8536	18.9
Graphite Epoxy	.063	.04	1.9	3265	724	4465 (350°) 4926 (260°)	8455 8915	18.7 19.8
Graphite Polyimide	.057	.049	2.522	3923	1438	4003	9364	20.8

Table 6. Aerobrake total structure mass and TPS mass for an isogrid structure.

Material	Face sheet and rib density lb/in ³	I in ⁴	I-beam area in ²	Face sheet thickness in	Core depth in	Structure mass lb	Joint mass lb	TPS mass lb	Total Aerobrake mass lb	% of LTV total mass
Aluminum	.101	1.18	.87	.02	1.5	3890	920	4003	8813	19.5
SiCp-Al	.104	.7	.44	.02	1.093	3030	779	4003	7812	17.3
Graphite Epoxy	.063	2.01	1.6	.023	.894	3214	556	4495 (3500) 5049 (2600)	8265 8819	18.3 19.5

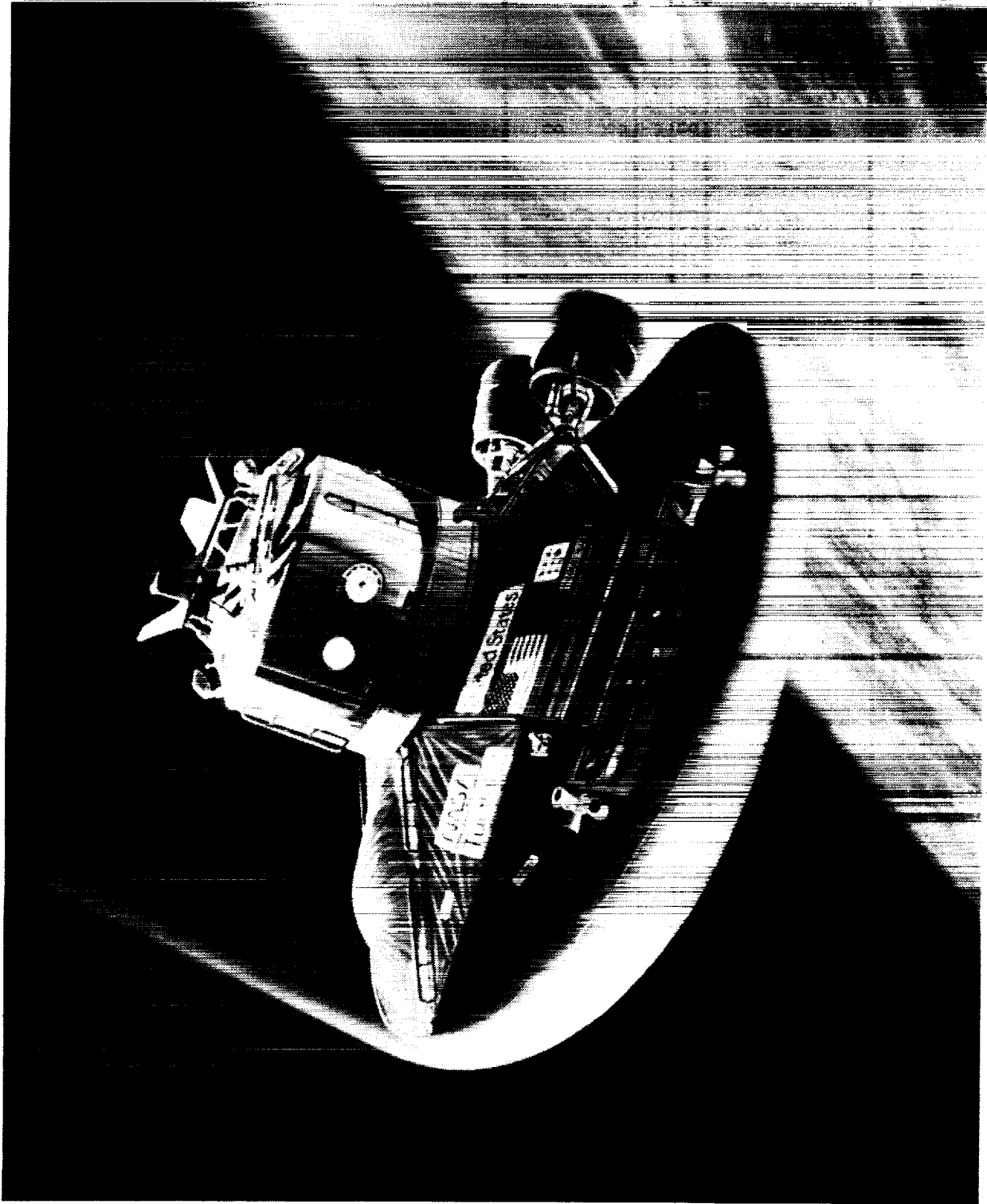


Figure 1. Lunar return transfer vehicle with aerobrace.

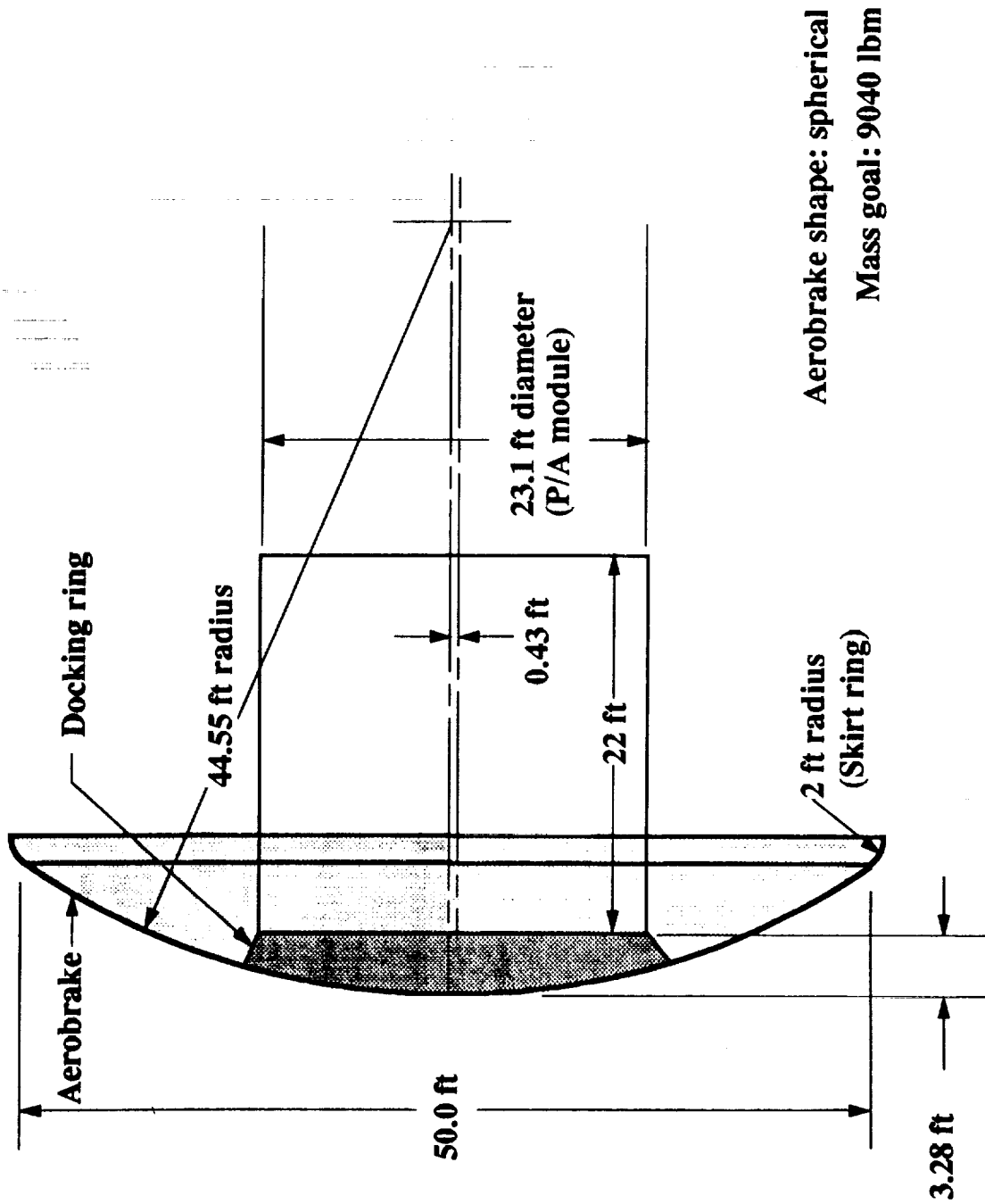


Figure 2. Aerobrake baseline geometry

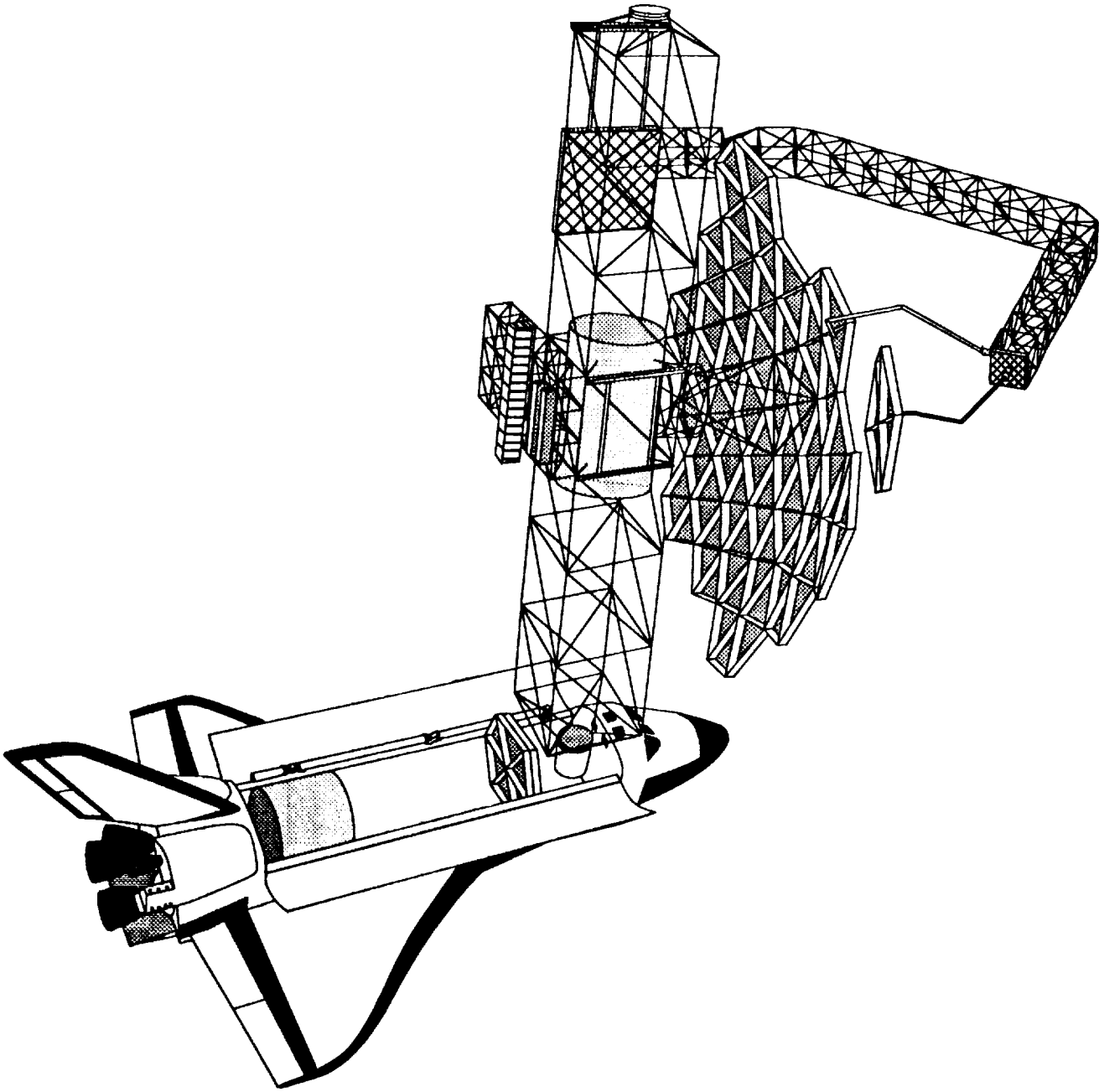
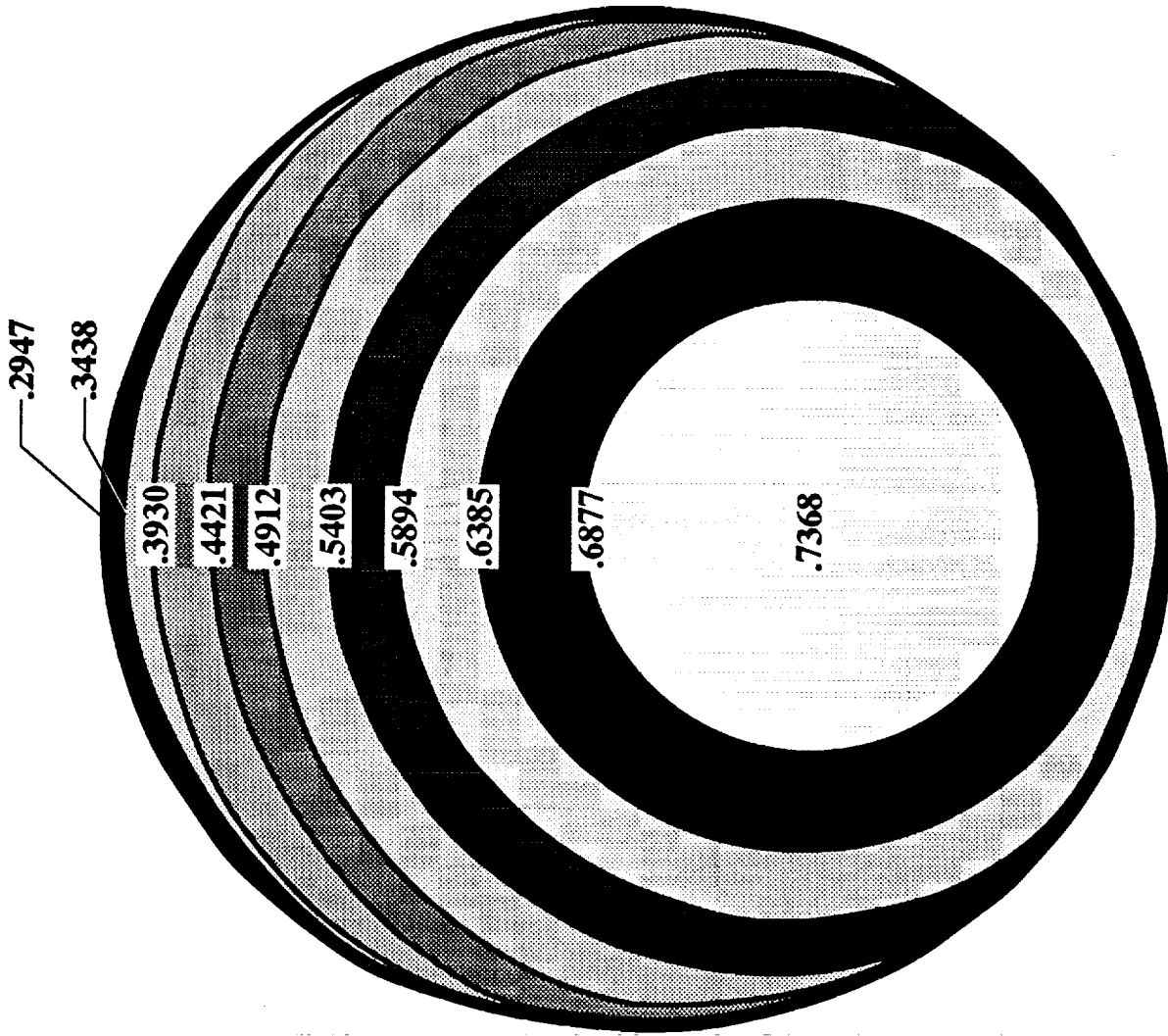
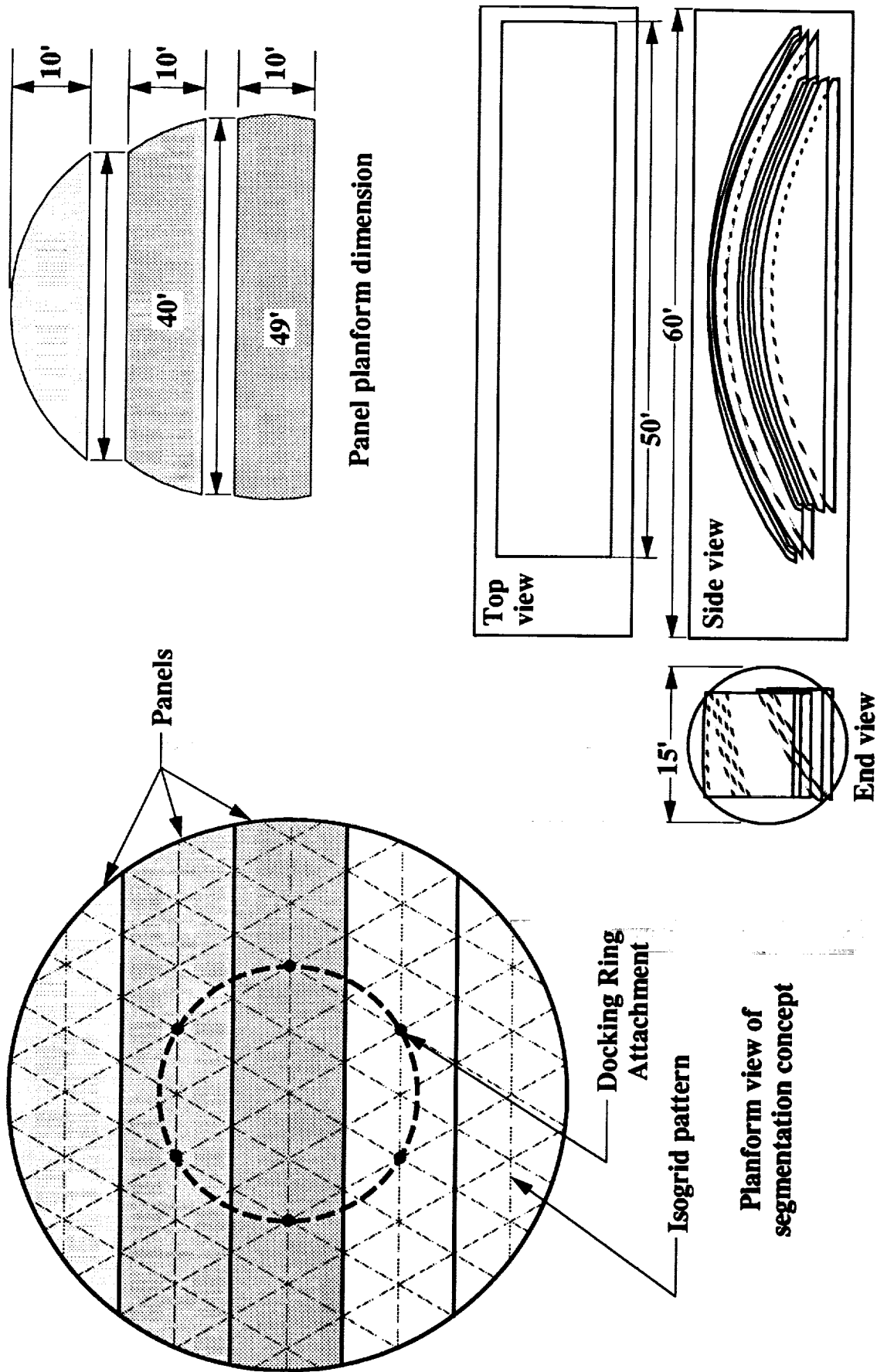


Figure 3. On-orbit assembly of an aerobrake from a Space Station-type platform.



Note: pressure in psi.

Figure 4. Aero brake pressure distribution.



Packaging configuration for STS cargo bay

Figure 5. Longitudinally sliced panels segmentation concept.

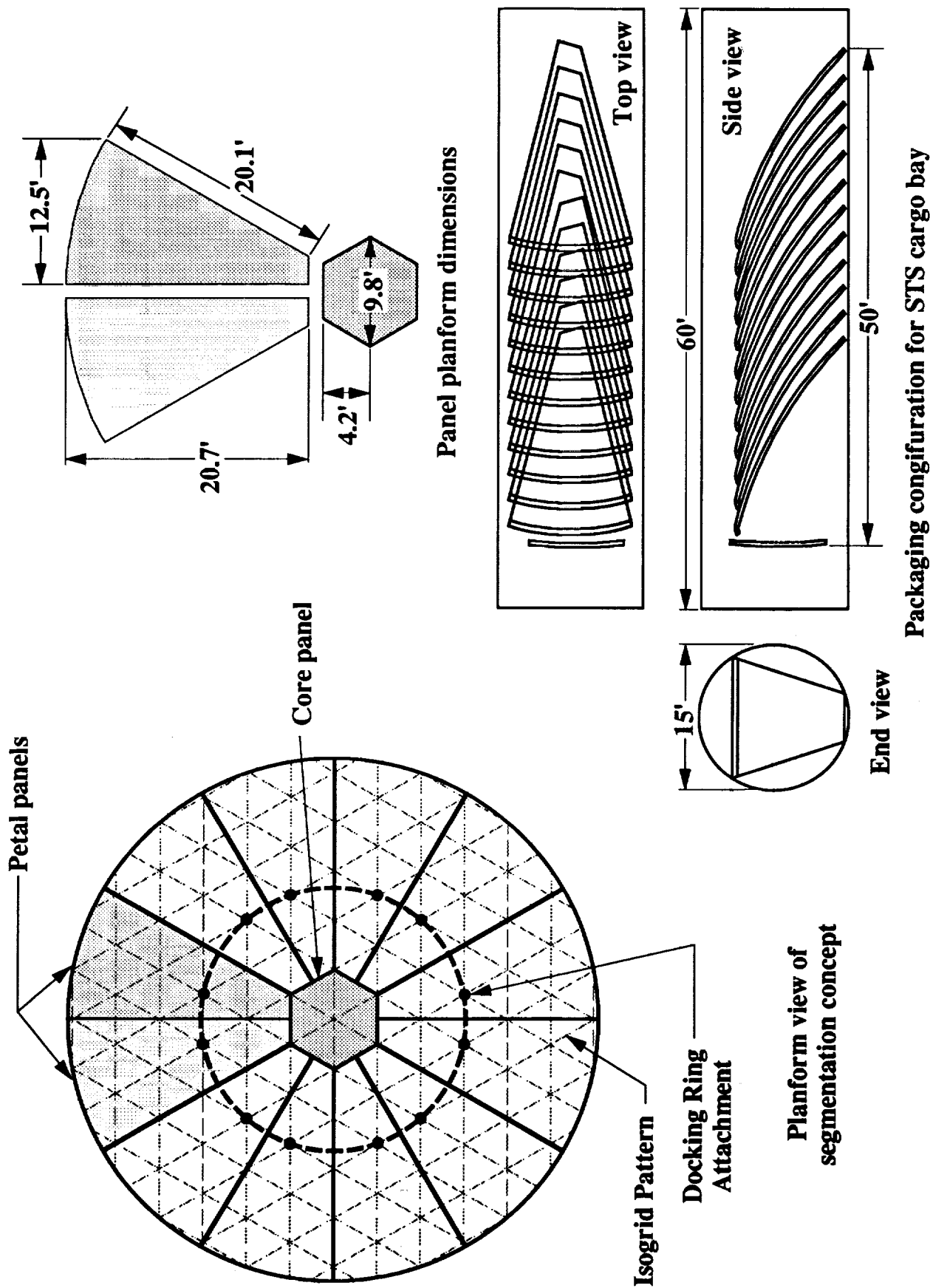


Figure 6. Core-petal panel segmentation concept.

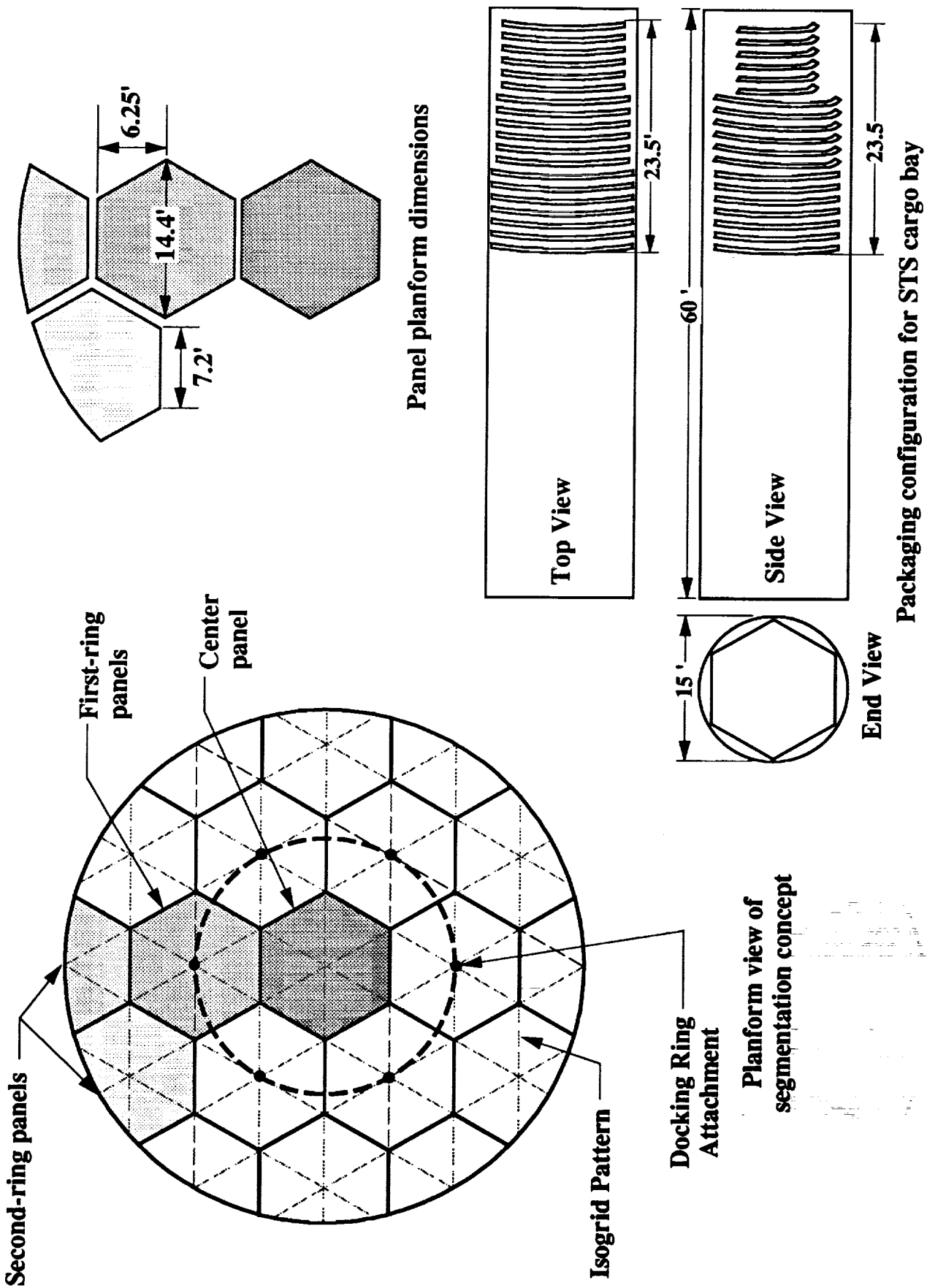
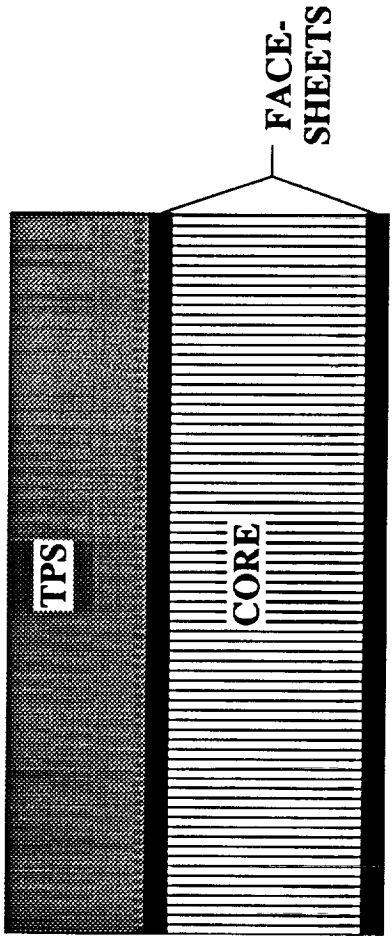
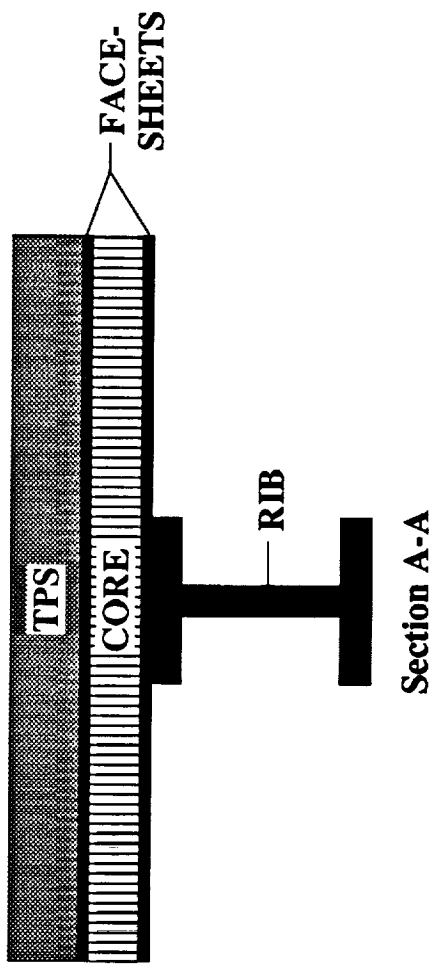
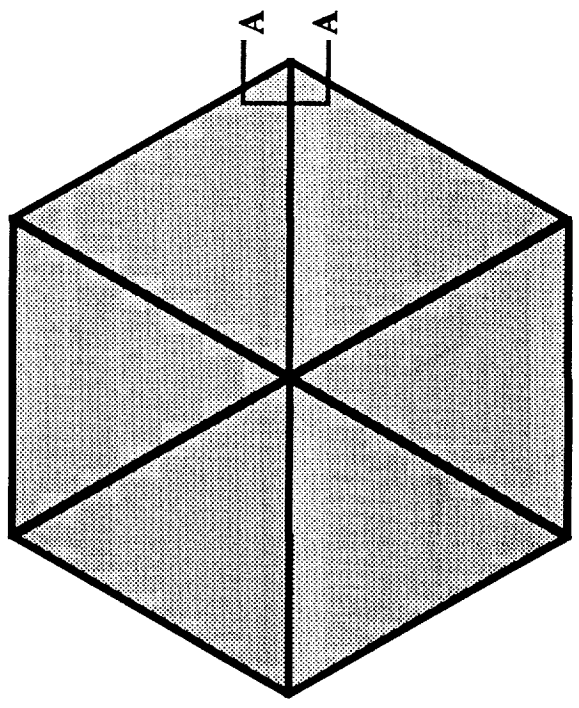


Figure 7. Hexagonal panel segmentation concept.



a. Sandwich concept.



b. Isogrid concept.

Figure 8. Structural concepts.

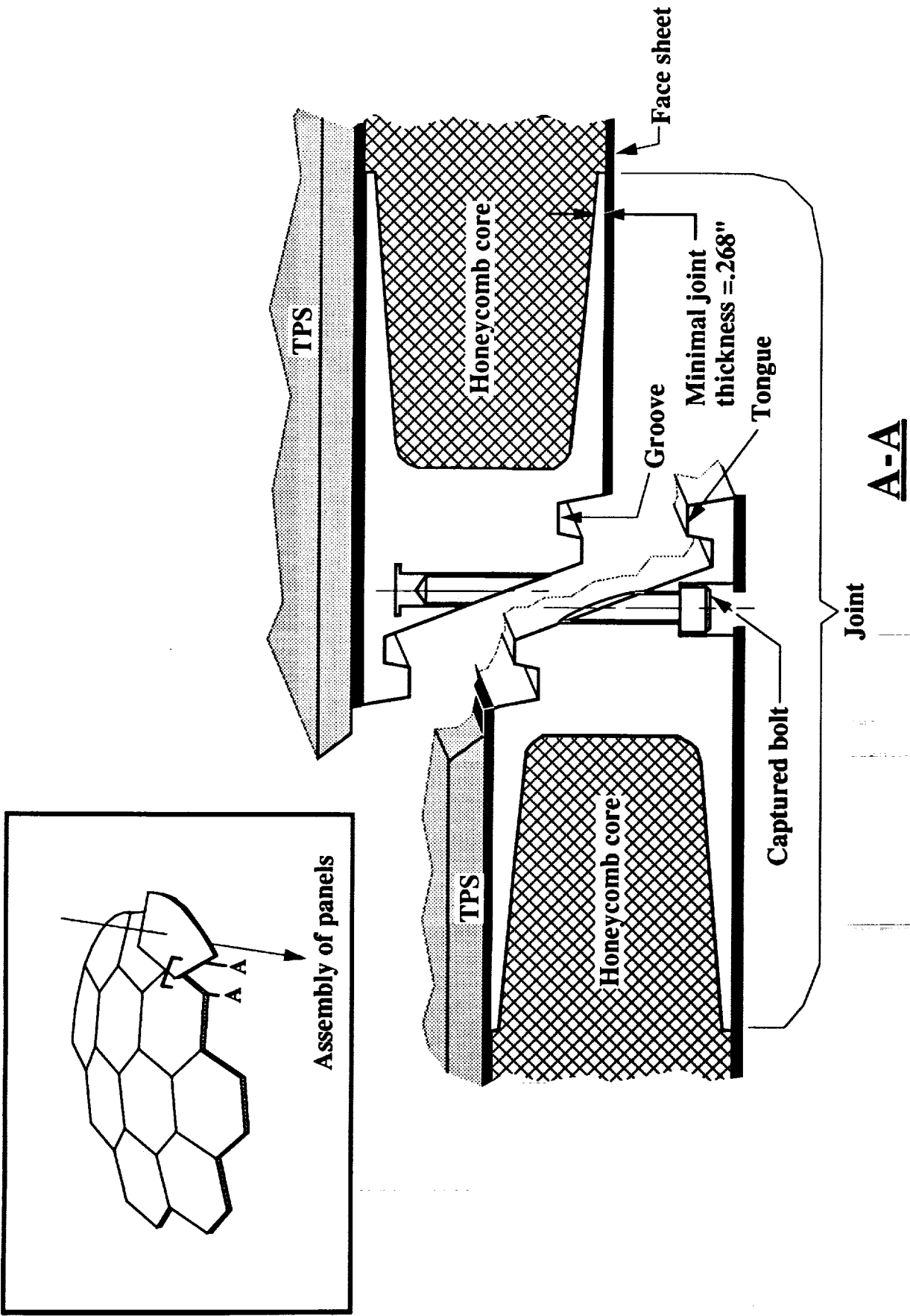


Figure 9. Line joint concept for sandwich panel and isogrid skin assembly.

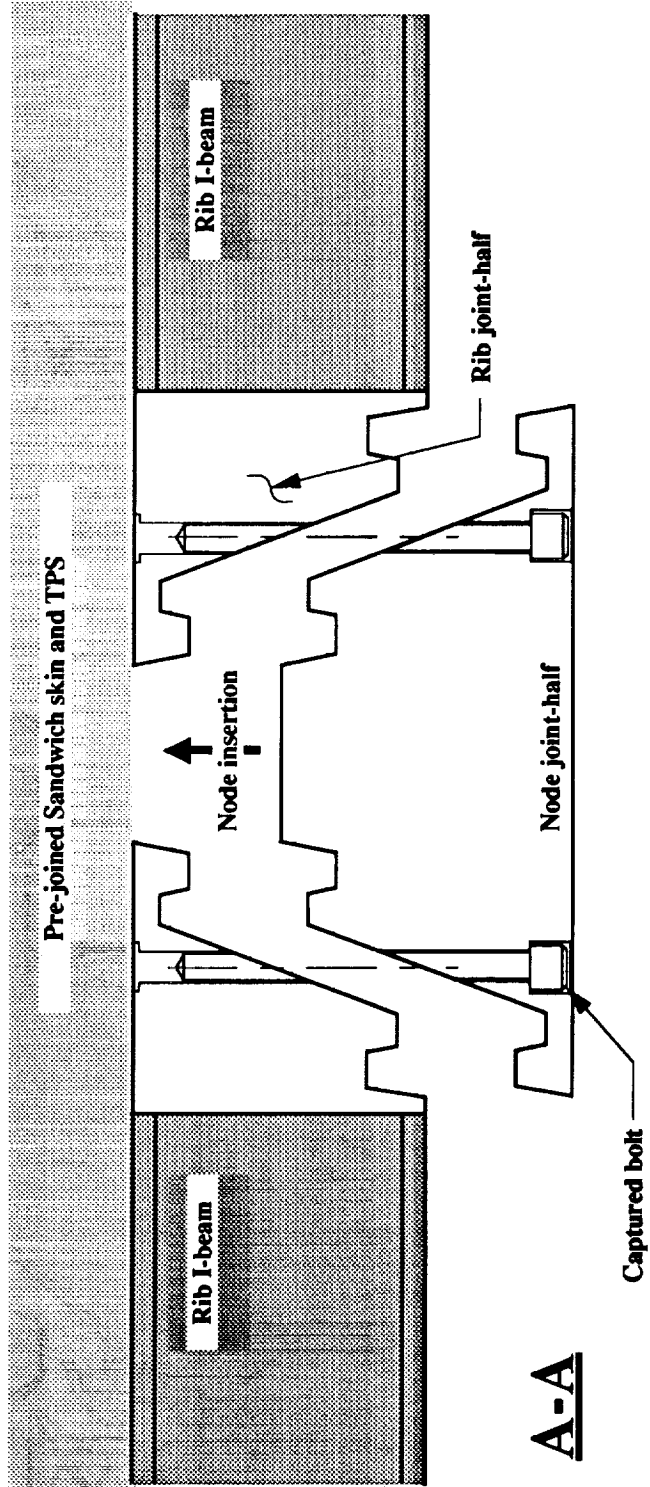
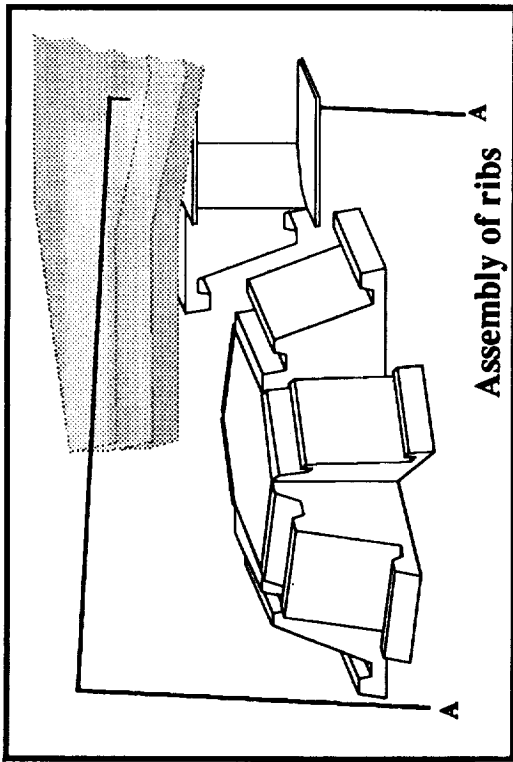


Figure 10. Rib-joint concept for isogrid rib assembly.

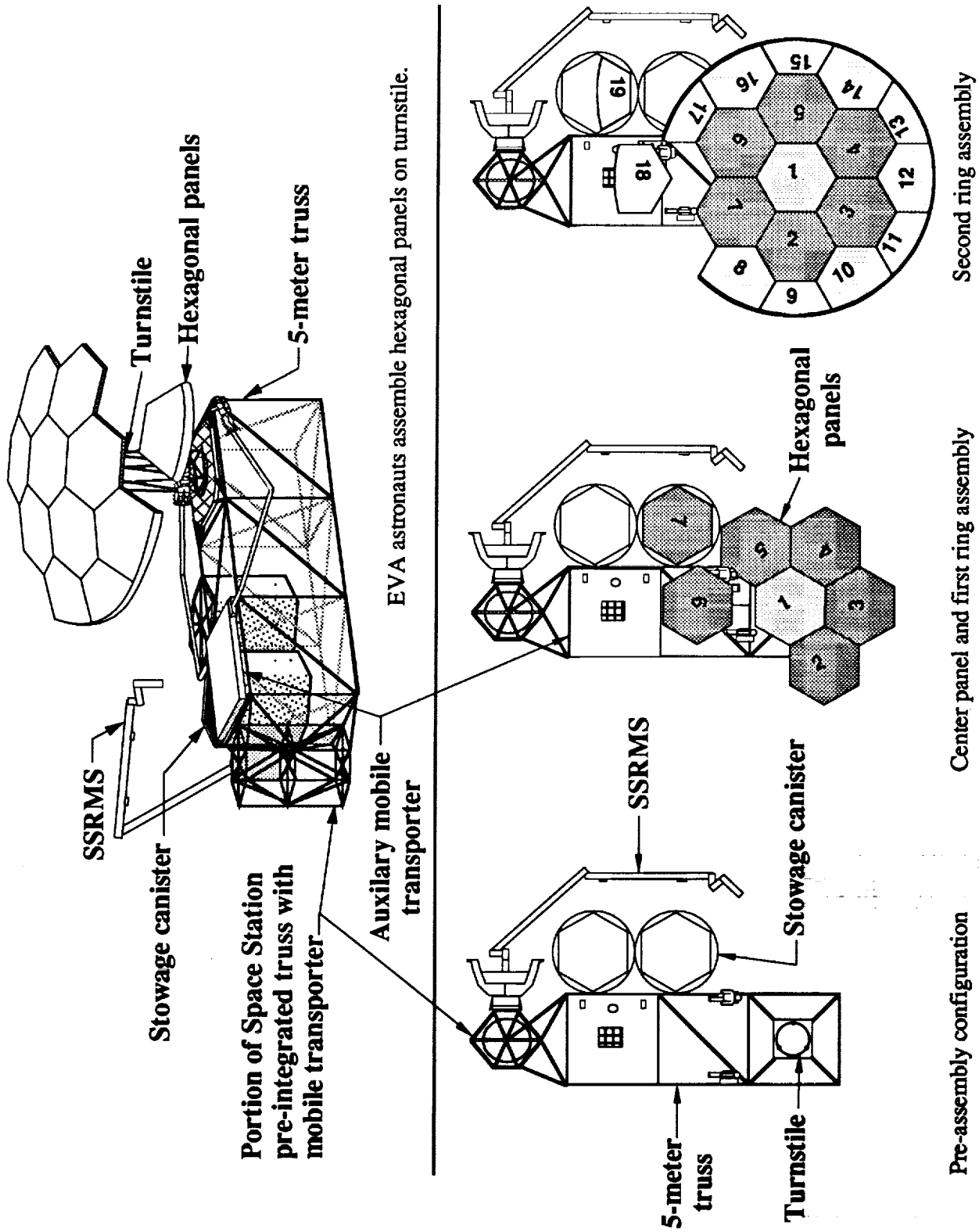


Figure 11. Hexagonal panel assembly procedure.

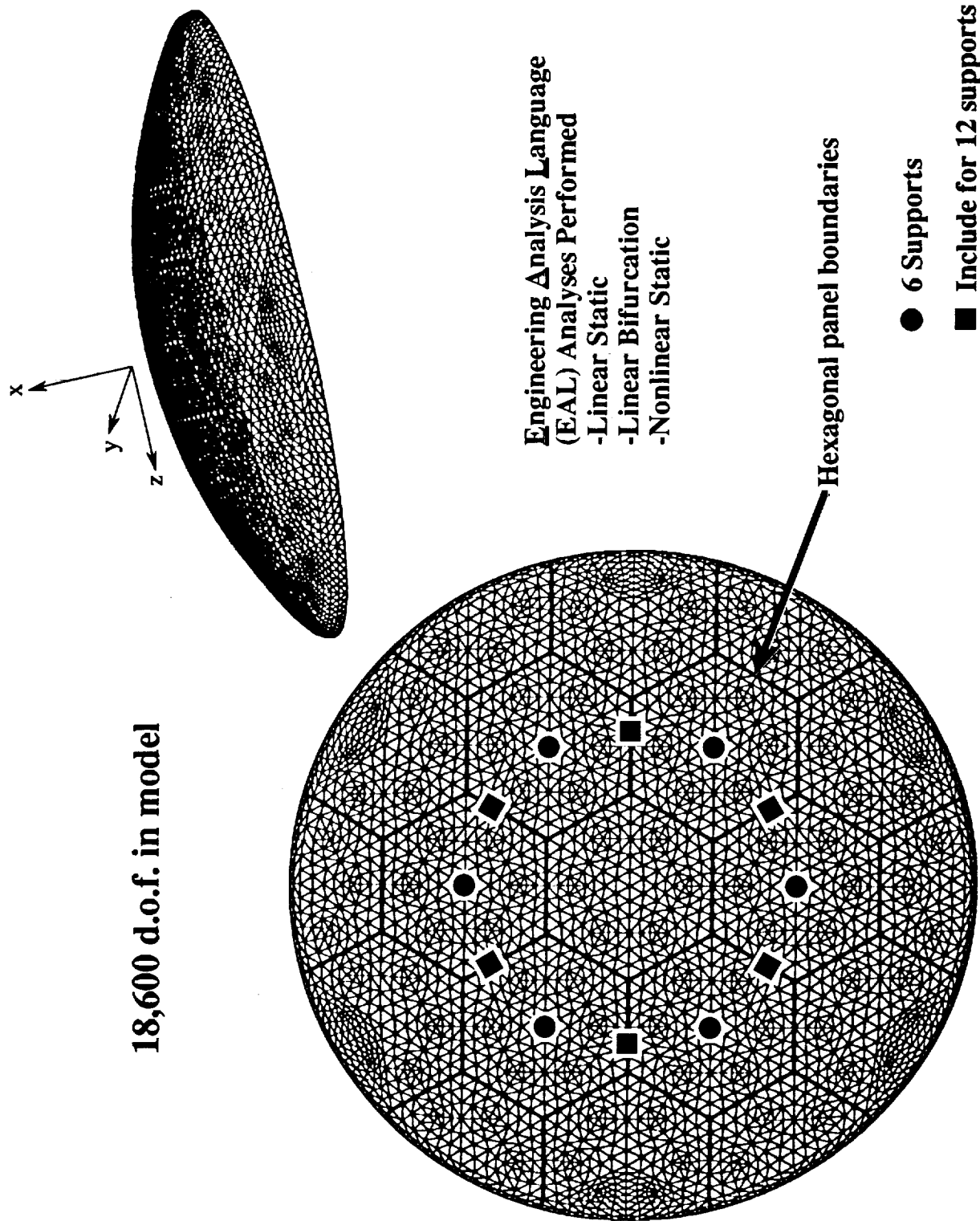


Figure 12. Finite element analysis model.

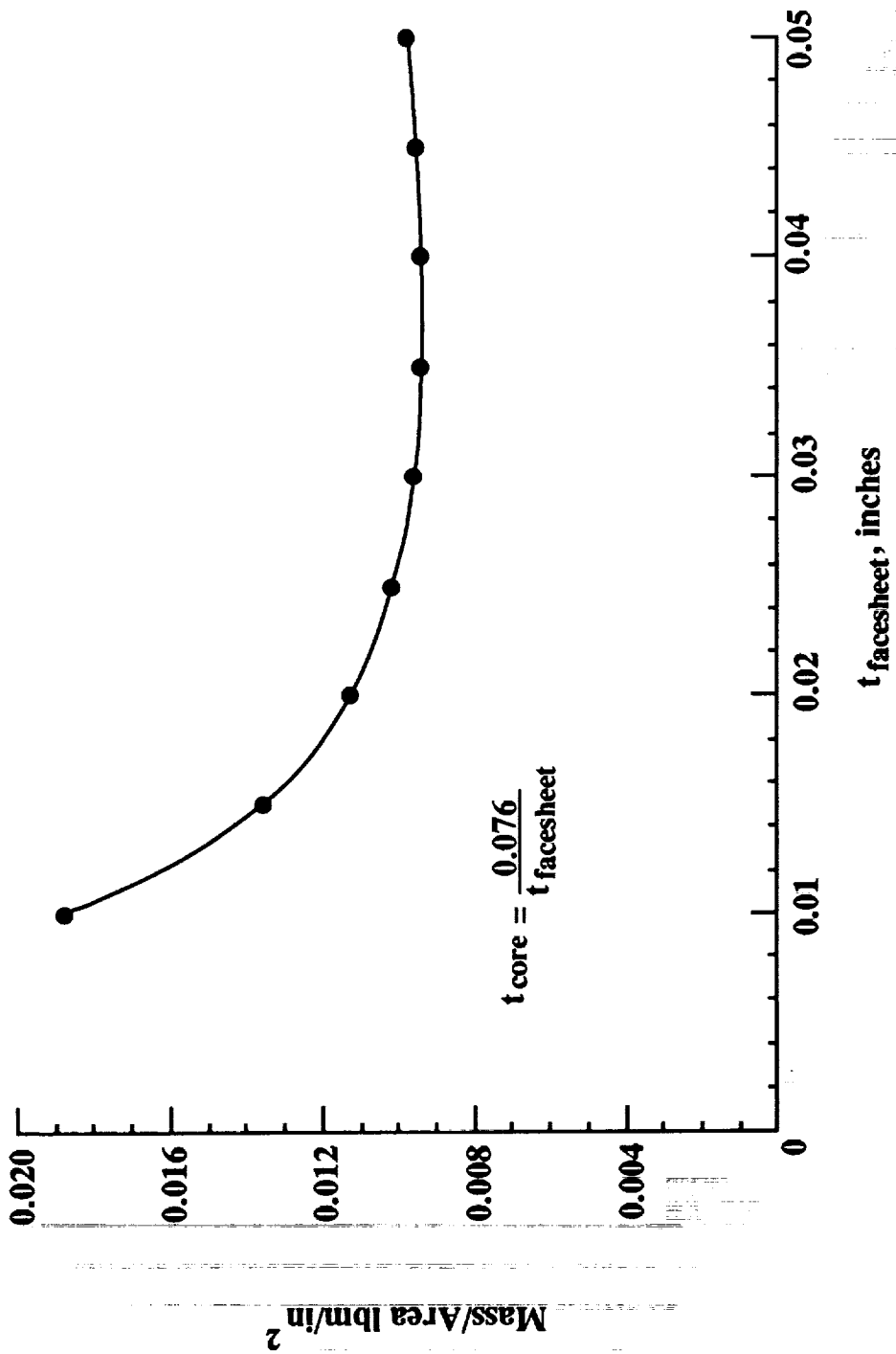


Figure 13. Sandwich concept; minimum mass for buckling.

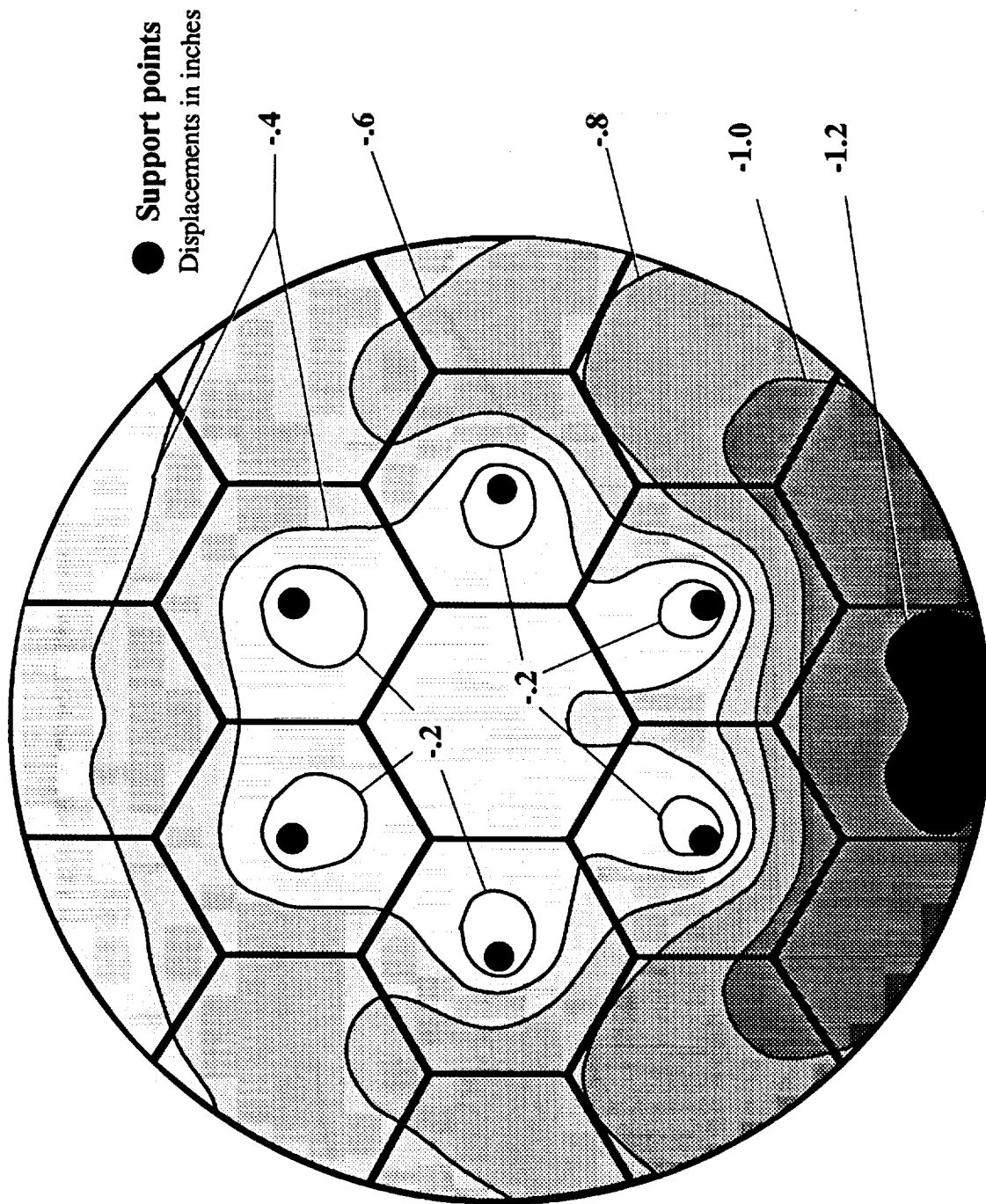
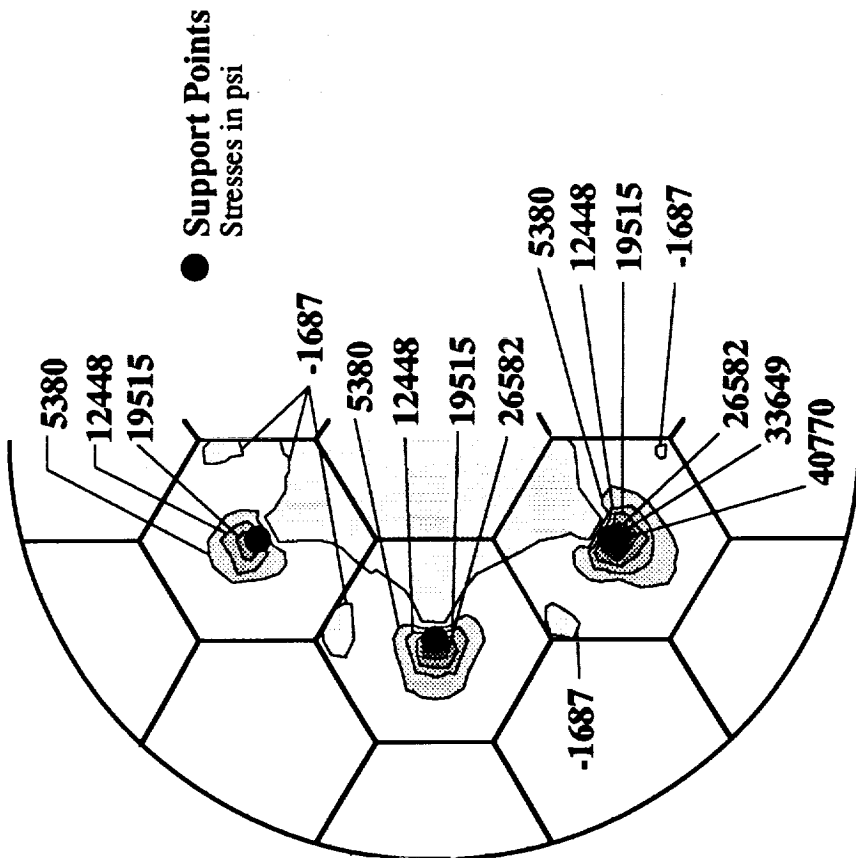
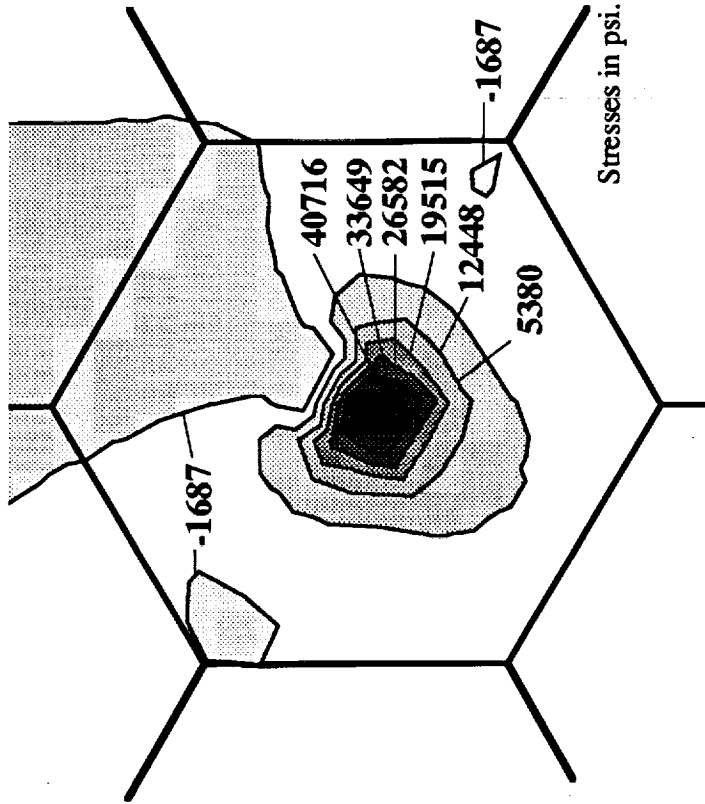


Figure 14. Sandwich concept x-displacement contour.



a. Stress contour.



b. Stress contour in vicinity of support point.

Figure 15. Typical sandwich facesheet σ stress contour.

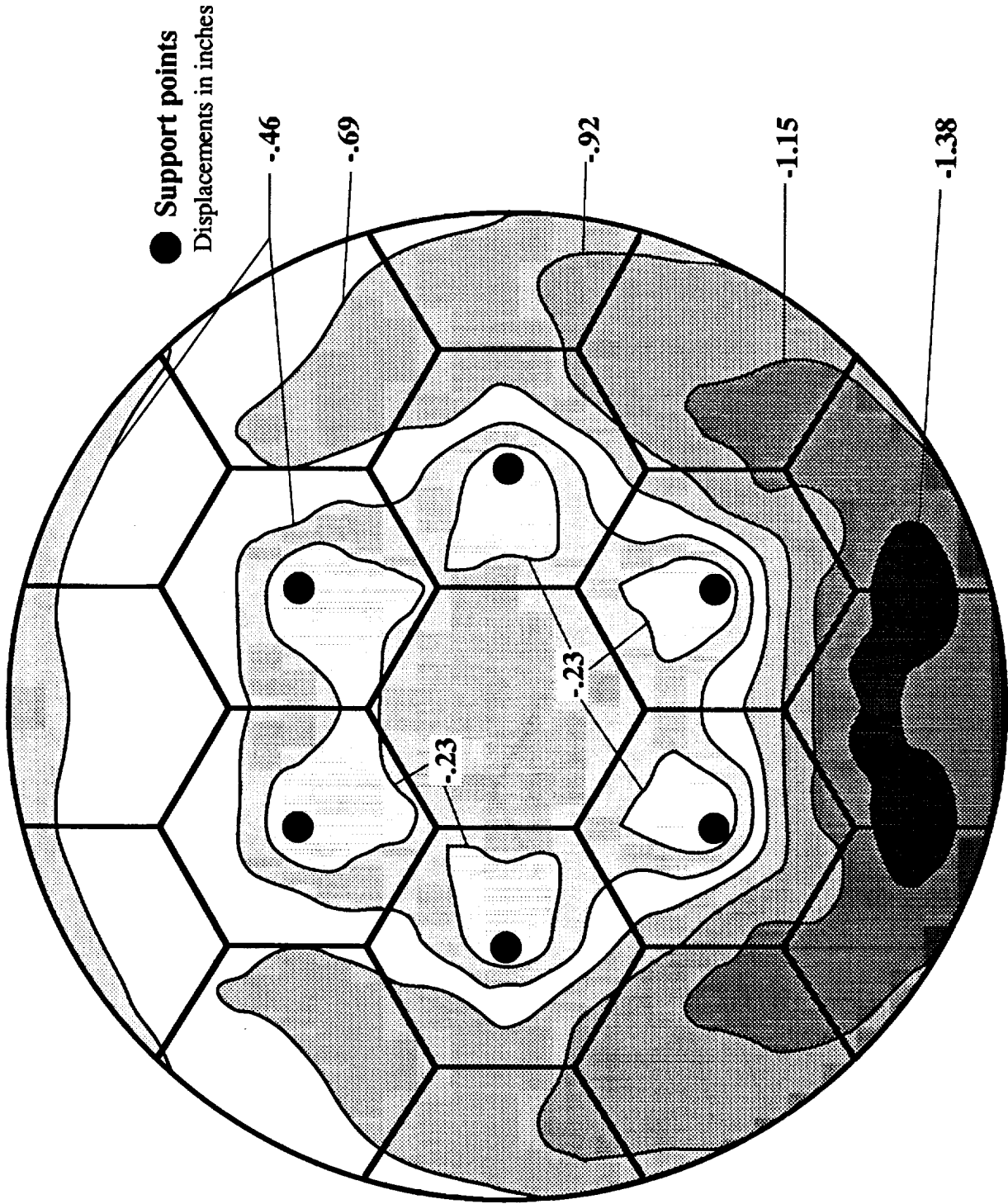


Figure 16. Isogrid concept x-displacement contour.

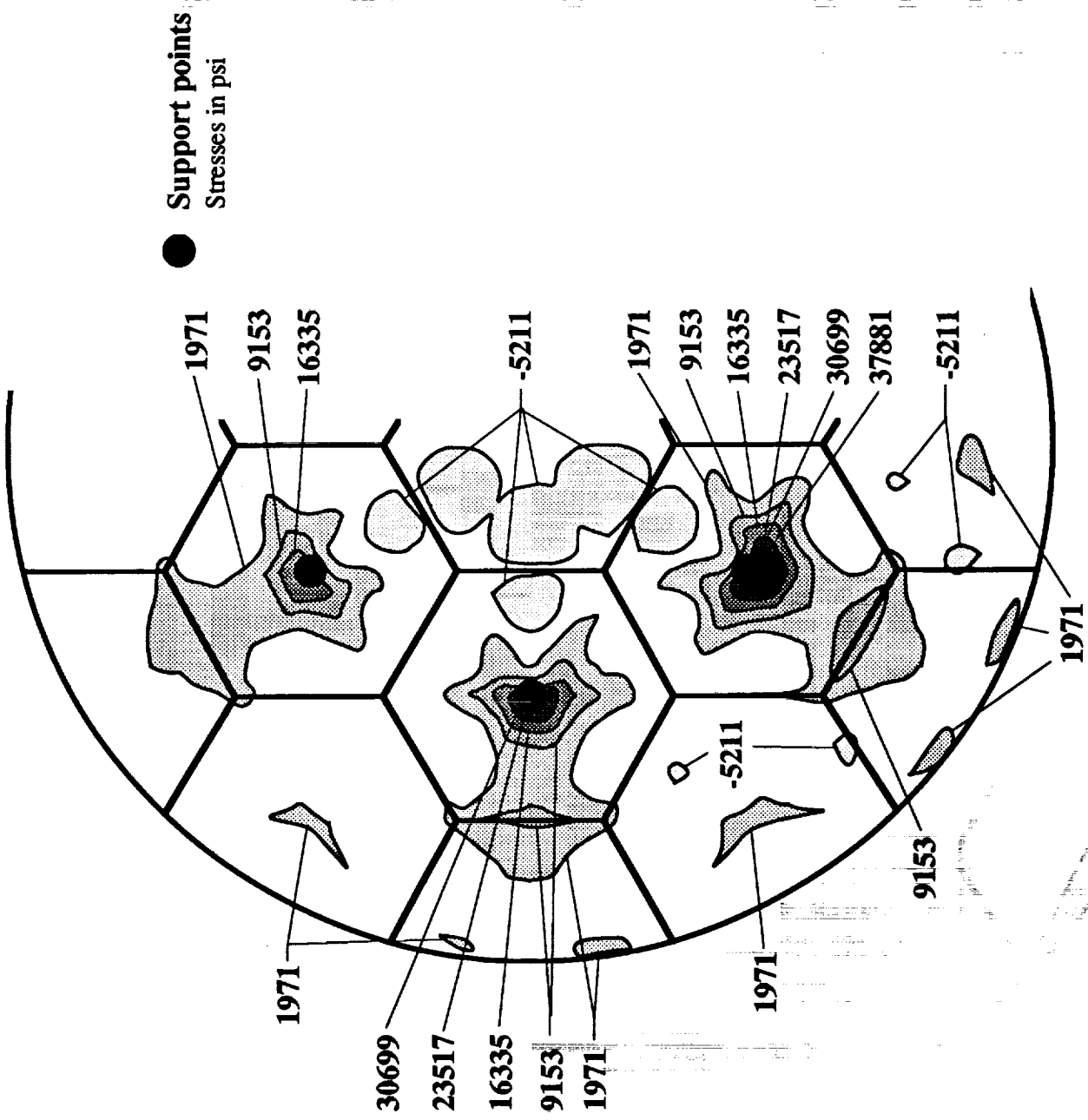


Figure 17. Typical isogrid skin σ_r stress contour.



REPORT DOCUMENTATION PAGE

Form Approved
OMB No. 0704-0188

Public reporting burden for this collection of information is estimated to average 1 hour per response, including the time for reviewing instructions, searching existing data sources, gathering and maintaining the data needed, and completing and reviewing the collection of information. Send comments regarding this burden estimate or any other aspect of this collection of information, including suggestions for reducing this burden, to Washington Headquarters Services, Directorate for Information Operations and Reports, 1215 Jefferson Davis Highway, Suite 1204, Arlington, VA 22202-4302, and to the Office of Management and Budget, Paperwork Reduction Project (0704-0188), Washington, DC 20503.

1. AGENCY USE ONLY (Leave blank)		2. REPORT DATE October 1993	3. REPORT TYPE AND DATES COVERED Technical Memorandum	
4. TITLE AND SUBTITLE Minimum Accommodation for Aerobrake Assembly-Phase II Final Report Structural Concepts for a Lunar Transfer Vehicle Aerobrake Which Can Be Assembled On Orbit			5. FUNDING NUMBERS WU 506-43-41-02	
6. AUTHOR(S) John T. Dorsey, Judith J. Watson, and Robin D. Tutterow				
7. PERFORMING ORGANIZATION NAME(S) AND ADDRESS(ES) NASA Langley Research Center Hampton, VA 23681-0001			8. PERFORMING ORGANIZATION REPORT NUMBER	
9. SPONSORING / MONITORING AGENCY NAME(S) AND ADDRESS(ES) National Aeronautics and Space Administration Washington, DC 20546-0001			10. SPONSORING / MONITORING AGENCY REPORT NUMBER NASA TM-107610	
11. SUPPLEMENTARY NOTES				
12a. DISTRIBUTION / AVAILABILITY STATEMENT Unclassified - Unlimited Subject Category - 18			12b. DISTRIBUTION CODE	
13. ABSTRACT (Maximum 200 words) A multidisciplinary conceptual study was conducted to define a reusable Lunar transfer vehicle (LTV) aerobrake which could be launched on a Space Shuttle of Titan IV and assembled on orbit at Space Station Freedom. A major objective of this study was to design an aerobrake, with integrated structure and thermal protection systems, which has a mass less than 20 percent (9040 lb) of the LTV lunar return mass. This paper describes the aerobrake segmentation concepts, the structural concepts, a joint concept for assembly, and a structural design with analysis of the aerobrake. Results show that a 50-foot diameter LTV aerobrake can be designed for on-orbit assembly which will achieve the 20 percent mass budget.				
14. SUBJECT TERMS Aerobrake; Structures; Sandwich Structure; Isogrid Structure; On-Orbit Assembly			15. NUMBER OF PAGES 37	
			16. PRICE CODE A03	
17. SECURITY CLASSIFICATION OF REPORT Unclassified	18. SECURITY CLASSIFICATION OF THIS PAGE Unclassified	19. SECURITY CLASSIFICATION OF ABSTRACT Unclassified	20. LIMITATION OF ABSTRACT	